



**QUEEN'S
UNIVERSITY
BELFAST**

Sea-level changes in Iceland and the influence of the North Atlantic Oscillation during the last half millennium

Saher, M. H., Gehrels, W. R., Barlow, N. L. M., Long, A. J., Haigh, I. D., & Blaauw, M. (2015). Sea-level changes in Iceland and the influence of the North Atlantic Oscillation during the last half millennium. *Quaternary Science Reviews*, 108, 23-36. <https://doi.org/10.1016/j.quascirev.2014.11.005>

Published in:
Quaternary Science Reviews

Document Version:
Peer reviewed version

Queen's University Belfast - Research Portal:
[Link to publication record in Queen's University Belfast Research Portal](#)

Publisher rights

© 2015 Elsevier Ltd. All rights reserved.

This is an open access article published under a Creative Commons Attribution-NonCommercial-NoDerivs License (<https://creativecommons.org/licenses/by-nc-nd/4.0/>), which permits distribution and reproduction for non-commercial purposes, provided the author and source are cited.

General rights

Copyright for the publications made accessible via the Queen's University Belfast Research Portal is retained by the author(s) and / or other copyright owners and it is a condition of accessing these publications that users recognise and abide by the legal requirements associated with these rights.

Take down policy

The Research Portal is Queen's institutional repository that provides access to Queen's research output. Every effort has been made to ensure that content in the Research Portal does not infringe any person's rights, or applicable UK laws. If you discover content in the Research Portal that you believe breaches copyright or violates any law, please contact openaccess@qub.ac.uk.

Open Access

This research has been made openly available by Queen's academics and its Open Research team. We would love to hear how access to this research benefits you. – Share your feedback with us: <http://go.qub.ac.uk/oa-feedback>

1 Sea-level changes in Iceland and the influence of the North Atlantic Oscillation
2 during the last half millennium

3 Margot H. Saher^{1*}, W. Roland Gehrels², Natasha L.M. Barlow³, Antony J. Long³, Ivan D.
4 Haigh⁴ and Maarten Blaauw⁵

5
6¹School of Ocean Sciences, Bangor University, Menai Bridge LL59 5AB, UK; ²Environment
7Department, University of York, Heslington, York YO10 5DD, UK; ³ Department of
8Geography, Durham University, South Road, Durham DH1 3LE, UK; ⁴Ocean and Earth
9Science, National Oceanography Centre, University of Southampton, European Way
10Southampton, SO14 3ZH, UK; ⁵School of Geography, Archaeology and Palaeoecology,
11Queen's University Belfast, Elmwood Avenue, Belfast BT7 1NN, UK.

12*Corresponding author (email: m.saher@bangor.ac.uk, tel: 0044 1248 383819, fax: 0044
131248 716367)

14

15**Abstract**

16We present a new, diatom-based sea-level reconstruction for Iceland spanning the last ~500
17years, and investigate the possible mechanisms driving the sea-level changes. A sea-level
18reconstruction from near the Icelandic low pressure system is important as it can improve
19understanding of ocean-atmosphere forcing on North Atlantic sea-level variability over multi-
20decadal to centennial timescales. Our reconstruction is from Viðarhólmi salt marsh in
21Snæfellsnes in western Iceland, a site from where we previously obtained a 2000-yr record
22based upon less precise sea-level indicators (salt-marsh foraminifera). The 20th century part of

23our record is corroborated by tide-gauge data from Reykjavik. Overall, the new
24reconstruction shows ca. 0.6 m rise of relative sea level during the last four centuries, of
25which ca. 0.2 m occurred during the 20th century. Low-amplitude and high-frequency sea-
26level variability is super-imposed on the pre-industrial long-term rising trend of 0.65 m per
271000 years. Most of the relative sea-level rise occurred in three distinct periods: AD 1620-
281650, AD 1780-1850 and AD 1950-2000, with maximum rates of $\sim 3 \pm 2$ mm/yr during the
29latter two of these periods. Maximum rates were achieved at the end of large shifts (from
30negative to positive) of the winter North Atlantic Oscillation (NAO) Index as reconstructed
31from proxy data. Instrumental data demonstrate that a strong and sustained positive NAO (a
32deep Icelandic Low) generates setup on the west coast of Iceland resulting in rising sea
33levels. There is no strong evidence that the periods of rapid sea-level rise were caused by
34ocean mass changes, glacial isostatic adjustment or regional steric change. We suggest that
35wind forcing plays an important role in causing regional-scale coastal sea-level variability in
36the North Atlantic, not only on (multi-)annual timescales, but also on multi-decadal to
37centennial timescales.

38

39Key words: diatoms, ocean dynamics, Iceland, Little Ice Age, sea-level rise, NAO

40

41

43Determining the nature and causes of sea-level variability in the pre-industrial era provides a
44long-term context for comparing recent sea-level trends and for developing future projections
45(e.g. Barlow et al., 2012; Gehrels et al., 2004; Kemp et al., 2011; Milne et al., 2009; van de
46Plassche, 2000). Driving mechanisms of sea-level changes include mass changes in land-
47based ice, and other processes such as steric expansion and contraction, and dynamic
48oceanographic processes including variations in wind stress and atmospheric pressure
49(Gehrels and Woodworth, 2013).

50Unravelling the relative importance of these processes on multi-decadal to centennial
51timescales requires the development of precise proxy-based sea-level reconstructions that
52extend before the start of instrumental observations, with good age (decadal) and height (sub-
53decimetre) control. In the North Atlantic, the most precise reconstructions are developed
54along low-energy coastlines with small tidal ranges where organic-rich salt marshes provide
55environments that are suitable for developing continuous sea-level records over the last few
56millennia (e.g. Gehrels et al., 2005; Kemp et al., 2011).

57Identifying the drivers of regional sea-level change demands multiple observations from
58different parts of any particular ocean basin, which by necessity will be from a variety of
59depositional and tidal range environments (Long et al., 2014). A variety of microfossil types
60that include foraminifera, testate amoebae and diatoms are typically used, on their own or
61occasionally in combination, to constrain palaeomorph surface elevations and past sea-level
62changes (e.g. Gehrels et al., 2001; Kemp et al., 2009; Charman et al., 2010; Barlow et al.,
632013).

64In this paper we develop a new relative sea-level (RSL) reconstruction from a meso-tidal salt
65marsh in western Iceland, an area particularly susceptible to wind-driven sea-level variability

66due to its location in the pathway of low pressure systems. In a previous paper Gehrels et al.
67(2006) reconstructed a 2000-yr record from this site using foraminifera (Fig. 1), and
68identified a single acceleration in sea level that was dated to the beginning of the nineteenth
69century. However, the record was heavily dominated by the upper marsh species *Jadammina*
70*macrescens* with occasional *Paratrochammina* (*Lepidoparatrochammina*) *haynesi*. This low
71species diversity provided limited constraints on the elevation of the formation of the past
72marsh surface, making it impossible to identify any fluctuations in relative sea-level change
73beyond the 19th century inflection. Here we revisit the study site, Viðarhólmi salt marsh, and
74focus in on the last five centuries. We exploit the greater sensitivity to elevation (and hence
75sea level) of diatoms to produce a ~500-yr sea-level reconstruction of high vertical precision.
76We also apply new chronological analyses to the upper part of the stratigraphic section
77previously studied to generate an improved age model using new tephra and AMS¹⁴C dates,
78in combination with previous AMS¹⁴C, ¹³⁷Cs and chemostratigraphical analyses. The resulting
79reconstruction identifies three distinct periods of rapid sea-level rise during the last ~500
80years.

81To assess the potential drivers behind these changes we compare the new record to proxy and
82instrumental reconstructions of the North Atlantic Oscillation (NAO) Index over the same
83interval. The NAO exerts a strong influence over regional wind patterns, precipitation and
84temperature, mainly in the winter (e.g. Hurrell et al., 2003). The influence of (winter) NAO
85(wNAO) on Atlantic sea level during the instrumental era is well established (Andersson,
862002; Haigh et al., 2010; Kolker and Hameed, 2007; Miller and Douglas, 2007; Tsimplis et
87al., 2005, 2006; Woodworth et al., 2007; Woolf et al., 2003), but its significance in controlling
88dynamic sea-level variability over longer time intervals has not previously been explored. In
89this paper we present proxy evidence of at least two pre-industrial oscillations in sea level
90that broadly correlate to changes in reconstructed wNAO in the North Atlantic Ocean,

91highlighting the influence of ocean-atmosphere forcing on regional-scale sea-level variability
92during past centuries.

932 Study area

94Viðarhólmi salt marsh (64.77°N, 22.42°W) is located on the west coast of Iceland (Fig. 1) in
95an area that has been seismically stable during the late Holocene (Angelier et al., 2004).
96Árnadóttir et al. (2009) estimate modest rates of uplift due to GIA (~1mm/yr) in the period
97AD 1993-2004 based on GPS observations, but Gehrels et al. (2006) documented 1.3 m of
98relative sea-level rise during the last 2000 years, indicating that on millennial time scales this
99coastal area is subsiding. The marsh is underlain by Tertiary basalt (Ward 1971), and
100protected by a barrier spit to the south and by an outcropping Holocene lava flow to the east.
101Several tidal channels dissect the salt marsh. Our fossil sediment section is taken from the
102cleaned face of one of these channels where a 2 m high peat section is exposed (Figs. 1, 2).
103This is the same section where monoliths for the Gehrels et al. (2006) study had been taken in
1042001 and 2003. Today the salt marsh is largely undisturbed by human influence but is
105occasionally grazed by sheep. Dominant plants on the marsh are *Carex lyngbyei*, *Agrostis*
106*stolonifera*, *Festuca rubra* and *Puccinellia maritima* (Ingólfsson, 1998). Mean tidal range at
107Viðarhólmi is 2.1 m, mean sea level (MSL) is 0.12 m above the Iceland geodetic datum and
108the highest astronomical tides reach ~2.1 m above MSL (Gehrels et al., 2006).

109Wind patterns in western Iceland are controlled by the position and strength of the Icelandic
110low pressure system which generally results in dominant wind directions from the east, with
111only rare westerlies (Einarsson, 1984). During positive phases of the NAO the Icelandic Low
112tends to deepen and is located further north than during negative phases (Serreze et al., 1997).
113In the 1930s, for example, the average position of the Icelandic low was at 61°N, while the

114 shift to a negative NAO mode from the 1940s to the 1970s was associated with a southward
115 movement of this low to around 59°N (Angell and Korshover, 1974). In addition, extra-
116 tropical cyclones tend to track along a more northerly path and are more frequent during a
117 positive NAO mode (Carleton, 1988).

1183 **Methods**

1193.1 Field and laboratory methods

120 In September 2009 we cleaned and re-sampled the upper 60 cm of section 3A of Gehrels et
121 al. (2006) using monolith tins driven into the cleaned sediment surface. The lithostratigraphy
122 of the marsh is detailed in Gehrels et al. (2006) and mainly comprises sandy peat (Fig. 2).
123 Sand- and silt-sized material in the section is of volcanic origin and includes tephra. Three
124 distinct horizons of silt are visible in the sequence at 54 cm, 34 cm and 14 cm. Section 3A
125 contains an orange-brown pumice at 58-60 cm, dated to 1226/7 (Gehrels et al., 2006), which
126 we used as the base of the re-sampled section.

127 We sampled modern diatoms from four transects across a height range of 0.74 m (35% of the
128 tidal range) from just above the Highest Astronomical Tide (HAT) to the coring site in the
129 lower part of the mid marsh at an elevation between Mean High Water Springs (MHWS) and
130 Mean High Water (MHW) (Fig. 1, Supplementary information Table 1). Surface samples
131 were collected with a cylindrical turf cutter. The top 1 cm was sub-sampled in the laboratory
132 for diatom analysis. Heights of sample sites were surveyed relative to geodetic and tidal
133 datums with a Total Station. Samples for diatom analysis were prepared using the techniques
134 detailed in Palmer and Abott (1986). Diatoms were identified using Foged (1974), Hartley et
135 al. (1996), Hemphill-Haley (1993), van der Werff and Huls (1957-1974) and classified by the
136 halobian classification system (Hustedt, 1953, Hemphill-Haley, 1993).

1373.2 Transfer functions

138 We applied a transfer function (Birks et al., 1990) based on present-day microfossil
139 assemblages to obtain estimates of palaeomarrow surface elevation from the down-core fossil
140 assemblages. Using detrended canonical correspondence analysis (DCCA) in CANOCO
141 version 4.5 (ter Braak and Smilauer, 2002) we calculated the length of the environmental
142 gradient of the modern diatom dataset at 2.2 standard deviation units. We therefore followed
143 the general rule of thumb that, because the DCCA gradient length is greater than 2 standard
144 deviation units, sufficient species in the training set have their optima located along the
145 environmental gradient and are collectively responding unimodally to elevation across the
146 marsh surface (ter Braak and Prentice, 1988). We developed a unimodal weighted averaging
147 partial least squared (WA-PLS) model (ter Braak and Juggins, 1993) using the software C²
148 (Juggins, 2003). We selected a WA-PLS model with two components ($r^2 = 0.75$, Root Mean
149 Squared Error of Prediction (RMSEP) = 0.09) as this provided a >10% improvement in r^2_{boot}
150 and RMSEP compared to a one component model. Adding further components did not
151 significantly improve model performance. The observed *versus* predicted marsh surface
152 elevations are shown in Fig. 3. The WA-PLS diatom model predicts the elevation of the core
153 top to within 1 cm.

154 We evaluated the similarity between the modern and fossil assemblages, and therefore the
155 robustness of our reconstructions, using the modern analogue technique (MAT) (Overpeck et
156 al., 1985; Jackson and Williams, 2004). We considered fossil samples with a minimum
157 dissimilarity coefficient (minDC) smaller than the 5th percentile as having a good analogue,
158 those with a minDC between the 5th and the 20th percentile as having a close analogue, and
159 those with a minDC of more than the 20th percentiles as having a poor modern analogue
160 (Simpson, 2007, Watcham et al., 2013). We removed all samples with a poor modern
161 analogue from our resulting RSL reconstructions.

1623.3 Chronology

163We added nine high-precision AMS¹⁴C dates (Bronk Ramsey et al., 2007), four bomb-spike
164AMS¹⁴C dates, and a tephra marker to the existing chronological data of Gehrels et al. (2006)
165(Table 1). The chronology of the 2006 record was based on conventional AMS ¹⁴C, ¹³⁷Cs,
166Pb/Li, ²⁰⁶Pb/²⁰⁷Pb and magnetic declination measurements. The new high-precision AMS ¹⁴C
167dates were obtained from fragile, horizontally embedded, detrital plant remains, and the
168exoskeletons of a (non-burrowing) weevil (*Otiorhynchus* sp.). These analyses were conducted
169at the NERC Radiocarbon Facility within the Scottish Universities Environmental Research
170Centre, East Kilbride, Scotland.

171Within the core we detected tephra that erupted in AD 1721 from the Katla volcano located
172ca. 200 km southeast of Viðarhólmi. This is an exceptional find because other historic Katla
173tephras (such as AD 1755) were transported by winds in a northeasterly direction and did not
174reach our field site (Haflidason et al., 2000). The original Gehrels et al. (2006) age model
175suggested that the Katla AD 1721 tephra (Larsen, 2000) could be located in the sampled
176sequence between 34 and 48 cm. We therefore targeted this depth range at 1 cm intervals,
177sieving samples and examining the 25-63 µm fraction under a light microscope. About 60
178tephra shards were picked from each sample, and prepared for electron probe analysis at the
179School of Geosciences, University of Edinburgh. We selected 154 grains on the basis of
180successful preparation and pristineness of the material, and analysed their chemical
181composition on a Cameca SX100 electron microprobe, with rhyolitic (Lipari) and basaltic
182(BCR2g) standards used for calibration (see Hayward, 2012). We identified 39 grains with
183Katla geochemistry (Einarsson et al., 1980; Óladóttir et al., 2008) (Supplementary
184Information Table 2), of which nine had the characteristic K₂O/P₂O₅ signature of historic
185Katla eruptions (Óladóttir et al., 2008). A maximum of five historic Katla grains per sample
186were found at 39 cm; all other samples contained one shard at most. On this basis we

187 assigned a date of AD 1721 to the level at 39 cm, assuming that bioturbation and
188 remobilisation by wind and water subsequently re-distributed some shards over a wider depth
189 range (e.g. Davies et al., 2007; Gehrels et al., 2008).

190 We developed our age-depth model (Fig. 3) using the Bacon package in R (Blaauw and
191 Christen, 2011). Bacon requires as input a prior mean accumulation rate which we calculated
192 using the depth of the AD 1226-7 pumice tephra at 58 cm (Gehrels et al., 2006; Hafliðason et
193 al., 1992; Sigurgeirsson 1992). In the 2001, 2003 and 2009 monoliths the pumice tephra was
194 found at 58 cm, suggesting negligible sedimentation between sample collection dates.

195 Although this does not allow us to reconstruct sea-level changes during the past decade, it
196 does enable all analyses to be easily combined into one chronology. The stratigraphy and our
197 age-depth model do not show evidence of other significant hiatuses in the record.

198 3.4 Sea-level reconstructions

199 We translated the palaeo-marsh elevations calculated by the transfer functions into relative
200 sea level (RSL) using the equation:

$$201 \text{RSL (m)} = \text{sample height (m MSL)} - \text{palaeo-marsh elevation (m MSL)} \text{ (e.g. Gehrels, 1999)}$$

202 Results are presented in Table 2. The sample-specific bootstrapped RMSEP gives the vertical
203 uncertainty (approximate to 1σ) for each fossil sample, although in the figures we multiplied
204 the errors by 1.96 to 2σ . All sample ages and errors are based on modelled ages; those from
205 dated levels have reduced uncertainties compared to those from intermediate (undated) levels.
206 On the basis of four ^{14}C -dated sea-level index points that directly overlie bedrock, Gehrels et
207 al. (2006) concluded that the section is free of any significant compaction. This is in
208 agreement with the compaction studies of Brain et al. (2012) who found that thin,

209lithologically homogeneous stratigraphies, like the one described here, are not significantly
210affected by compaction.

211To calculate error envelopes for our sea-level reconstruction we resampled the RSL data
212points in R using their individual age and vertical error estimates. For each of 1,000
213iterations, we sampled random values from the means and (1 standard deviation) errors of the
214age and RSL estimates (assuming normal distributions) and calculated smooth splines
215(smoothing parameter 0.8) through the resampled data points. From the resulting family of
2161,000 smooth splines, we calculated 68% confidence ranges every 5th year between AD 1500
217and 2000. We determined the corresponding rises based on the derivatives of the above
218smooth splines.

219

2204 **Results**

2214.1 Modern diatoms

222The modern diatom flora of Viðarhólmi salt marsh is diverse, but the 28 taxa with an
223abundance of >5% of the total diatom valves counted (TDV) exhibit a strong vertical
224zonation across the marsh (Fig. 5). Assemblages are dominated by the genus *Navicula*, with
225as most abundant species *N. ignota*, *N. cincta type*, and *N. salinarum*. Other abundant species
226are *Luticola mutica* and *Nitzschia filiformis*.

2274.2 Fossil diatoms

228Fossil diatoms (Fig. 6) in the lower part of the core (~45-55 cm) are characterised by
229relatively high percentages (up to 40% TDV) of freshwater species such as *Pinnularia*
230***borealis***. From ~45 cm upward, the fresh- to brackish-water taxon *Navicula cincta type*

231dominates, with a maximum abundance of 71% TDV at 27 cm. In the upper 10 cm, *Luticola*
232*mutica* increases in abundance (max. 34% TDV).

2334.3 Age-depth model

234The age model shows a gradual increase in sedimentation rate from ~0.2 mm/yr at the base of
235the sequence to 3 mm/yr near the top (Fig. 4). The sample-specific age uncertainties vary
236through the section: 95% uncertainty intervals are ~40 years between AD 1570-1650, ~20-30
237years between AD 1775-1895 and ~10-20 years in the periods AD 1650-1775 and AD 1895-
2381950. Age uncertainties are smallest (<10 years) from AD 1950 onwards. Age uncertainties of
239our sea-level reconstruction are smaller than those of the individual data points (Fig. 3) due to
240the Bayesian nature of the calculation. The Bayesian algorithms prohibit age-models with
241reversals, so that ages that are highly anomalous do not feature strongly in the final age
242model.

2434.4 Quantitative relative sea-level reconstructions

244We combine the reconstructed marsh surface elevations (Fig. 6) with the age-depth model
245(Fig. 4) to produce a new record of past RSL change (Fig. 7A). Figure 7B shows the amended
246sea-level reconstruction for the past 2000 years, including the older data points of Gehrels et
247al. (2006). The diatom-based transfer function predicts a palaeommarsh surface elevation for
248the new samples with close/good modern analogues of 1.84 to 2.03 m. This falls within the
249range of the palaeommarsh surface elevations independently estimated by the foraminifera
250results in Gehrels et al. (2006). The elevation estimates are primarily controlled by species
251*Navicula ignota*, *Fragilariforma virescens* and *Opephora marina*. Overall, the reconstruction
252shows a RSL rise of ~0.6 m in the last 500 years. Most of the sea-level rise appears to have
253occurred in three steps, with rapid rise in the 17th century, the late 18th to early 19th century
254and the 20th century.

255

2565 Discussion

2575.1 Comparison with other records

258 The diatom-based transfer function produces a robust reconstruction that lies within the error
259 bars of, and thus is corroborated by, the original foraminifera-based reconstruction from this
260 site (Gehrels et al., 2006; Fig. 1C). The high species diversity and species turnover of the
261 diatoms, similar to those found by Patterson et al. (2000) in British Columbia, Canada, reveal
262 several decadal-scale fluctuations in sea level not resolved in the original foraminifera-based
263 reconstruction. Despite samples with poor modern analogues, especially towards the base and
264 in the uppermost samples, we can resolve several sea-level fluctuations.

265 The pronounced RSL inflection at ~AD 1820 in the foraminifera-based reconstruction for
266 Viðarhólmi salt marsh (Gehrels et al., 2006) was largely due to an abrupt change in the
267 original age-depth model. Our new age model is smoother and as a result the rapid
268 acceleration is removed. The latter part of the record shows a good fit with the Reykjavik
269 tide-gauge record (Fig. 7A).

270 The overall rise in RSL identified in our new reconstruction (Fig. 7A) of 0.6 m during the last
271 ~500 years cannot be directly compared with global sea-level reconstructions, such as that of
272 Jevrejeva et al. (2006), as the latter is corrected for glacial isostatic adjustment (GIA). We do
273 not correct our record for GIA, as the best available data based on Global Positioning System
274 (GPS) data amounts to ~1 mm/yr uplift (Árnadóttir et al., 2009), which is not compatible with
275 the millennial-scale relative sea-level rise documented in the Viðarhólmi sediments (Gehrels
276 et al., 2006). We therefore instead focus on fluctuations in the sea-level record which may
277 provide clues for driving mechanisms.

278 Interestingly, the proxy RSL reconstructions from the eastern USA (Kemp et al., 2011, 2013),
279 Nova Scotia (Gehrels et al., 2005) and north-west Scotland (Barlow et al., 2014) show little
280 variability during the past millennium before a late 19th to early 20th century inflection. These
281 differences between the Icelandic and other North Atlantic records suggest that regional/local
282 influences play a significant role in driving sea-level variability.

283 5.2 West Icelandic sea level and NAO

284 The multi-decadal variability observed in our new Iceland record is reminiscent of the
285 fluctuations observed in the North Atlantic Oscillation (NAO) (e.g. Cornes et al., 2013;
286 Hurrell and van Loon, 1997; Jones et al., 1997; and Luterbacher et al., 1999). We therefore
287 first explore the relationship between the NAO and sea level in instrumental records, and then
288 test the hypothesis that the periods of rapid sea-level rise in our Icelandic salt-marsh proxy
289 record are synchronous with reconstructed changes in NAO.

290 The influence of the NAO on sea level has been established in different areas such as the
291 North Sea area (Wakelin et al., 2003) and the Baltic (Andersson, 2002). The NAO, which is
292 defined as the pressure difference between the Azores High and the Icelandic Low, can affect
293 Icelandic sea level through air pressure changes and wind stress. Air pressure will influence
294 sea level in its vicinity due to the inverted barometer effect which is $\sim 1\text{cm/mbar}$ (Ponte,
295 1992; Wunsch and Stammer, 1997); as air pressure rises (falls) so sea level falls (rises). The
296 annual average pressure recorded by the Stykkishólmur weather station ($\sim 40\text{ km}$ from our
297 field site; see Fig. 1) has varied by 12 mbar over the observational period (AD 1949-2012),
298 which would translate into sea-level fluctuations of $\sim 12\text{ cm}$. The NAO, however, is mainly a
299 winter phenomenon, and intra-annual variations in average winter (DJF) air pressure are
300 considerably larger at 26 mbar. Additionally, the Icelandic Low dominates the wind patterns

301in the vicinity of our field site, and this pressure system is also known to influence sea level
302(e.g. Douglas, 2008; Hong et al., 2000; Kolker and Hameed 2007).

303To evaluate the possible effect of NAO on west Icelandic sea level, we compare (Fig. 8A-D)
304annual mean relative monthly sea level (RMSL) records from Reykjavik, with time-series of
305air pressure, wind speed, and wind direction, averaged across a box encompassing our study
306area (see Fig 9), and the NAO index (<http://www.cru.uea.ac.uk/~timo/datapages/naoi.htm>).

307The time-series of air pressure, wind speed and wind direction were derived from MSL
308pressure and 10 m wind fields, obtained from the 20th century global reanalysis dataset
309(Compo et al 2011). These meteorological fields are available at a resolution of a data point
310every 6 hours from 1871 to 2011 and have a horizontal resolution of 2°. Data were
311downloaded from the reanalysis web page (http://www.esrl.noaa.gov/psd/data/20thC_Rean/).
312We generated both annual averages and winter (DJF) averages (Fig. 8A-D). To reduce the
313considerable year-to-year variability we applied a 9-year running average (Fig. 8E-H) to the
314derived time-series (which is similar to the resolution of our proxy sea-level record). As
315expected, there is a negative correlation between (9-year smoothed) air pressure and MSL
316(annual: $r^2=0.08$; winter: $r^2=0.27$), which is explained by the inverted barometer effect. There
317is a positive correlation between MSL (9-year smoothed) and wind direction (annual: $r^2=0.01$;
318winter: $r^2=0.26$). There is a stronger (positive) correlation between MSL (9-year smoothed)
319and the NAO (annual: $r^2=0.27$; winter: $r^2=0.53$); and wind speed (annual: $r^2=0.54$; winter:
320 $r^2=0.41$).

321To further compare the atmospheric circulation near Iceland with the Reykjavik tide-gauge
322record, we detrend the tide-gauge record (using a linear trend fitted to the complete MSL
323time-series) to remove lower-frequency variability such as that associated with changes in
324ocean volume. We subdivide the tide-gauge data into years in which MSL was $>+1sd$,

3250 <+1sd, 0>-1sd, and <-1sd, and calculate the average atmospheric patterns, over the period
326 AD 1871-2011, for these categories (Fig 9).

327 As noted above; the Icelandic Low, a persistent centre of low atmospheric pressure off the
328 west coast of Iceland, tends to be deeper when sea levels at Reykjavik are higher. The
329 dominant wind pattern involves strong winds from both the north and the south, resulting in a
330 weak (though still significant) correlation of wind direction with MSL, and a strong
331 correlation with wind strength. The combined wind domains generate set-up on the western
332 Icelandic coast.

333 The instrumental data reveal a strong correlation of NAO-related factors with instrumental
334 measurements of sea level. In order to evaluate a potential link between our ~500 year sea-
335 level record and wNAO we examined several proxy-based reconstructions of wNAO (Glueck
336 and Stockton, 2001; Cook et al., 2002; Luterbacher et al., 2002; Trouet et al., 2009). The
337 Glueck and Stockton (2001) record is based on data from GISP, and dendrochronological data
338 from Finland to represent the northern pole of the NAO, and many tree ring and precipitation
339 records from the southern pole. The records by Cook et al. (2002) and Luterbacher et al.
340 (2002) are both based on data from a plethora of sites on both sides of the Atlantic. The
341 Trouet et al. (2009) record is based on winter precipitation records from Scotland and
342 February-to-June drought records from Morocco. There are many reasons why proxy records
343 of the NAO may differ (see Trouet et al. (2012) for a review), but we consider the Trouet et
344 al. (2009) reconstruction to be most suitable for comparing with the Iceland sea-level record
345 due to its north-western European northern pole, and the position of Scotland in the dominant
346 wind patterns over the North Atlantic (Fig. 9).

347 In Figure 10 we calculate from our sea-level reconstruction (Fig. 10A) rates of sea-level
348 change (Fig. 10B) and identify three periods of rapid sea-level rise. We arbitrarily define

349 'rapid' as exceeding the average global sea-level rise during the 20th century (1.7mm/yr,
350 Church and White (2006)). The three periods are: AD 1620-1650, when sea-level rise peaked
351 at ~2 mm/yr, and AD 1780-1850 and AD 1950-2000, when maximum sea-level rise was ~3
352 mm/yr. (These figures are based on the most probable interpretation of the data – see section
353 3.4). A comparison with the Trouet et al. (2009) wNAO record (Fig. 10C) shows that the
354 three periods in which the rate of sea-level rise is highest are, within age error, synchronous
355 with strong shifts toward a more positive wNAO. These shifts are by far the largest within the
356 considered time period. Maximum rates of sea-level rise were achieved towards the end of
357 the NAO shifts. The most recent period of rapid sea-level rise (late 20th century) also
358 corresponds with strong shifts towards more positive wNAO in the records by Glueck and
359 Stockton (2001), Cook et al. (2002), and Luterbacher et al. (2002) (Supplementary Fig. 1).
360 Around AD 1800 Luterbacher et al. (2002) also record a marked increase in NAO index
361 (Supplementary Fig. 1). The earliest period of rapid sea-level rise does not seem to have a
362 corresponding signal in NAO records other than the one by Trouet et al. (2009), but others
363 have also found an increased correlation between Atlantic sea level and NAO in more recent
364 centuries (e.g. Andersson, 2002).

365 From resampling the Trouet et al. (2009) NAO record at the same resolution as a detrended
366 version of our RSL record (Supplementary Fig. 1B), which removes longer wavelength
367 components of sea level, we calculate a coefficient of 0.3 ($p=0.05$) for the correlation
368 between RSL at Viðarhólmi and the NAO (Fig. 11). This suggests a significant influence of
369 NAO on our ~500-year sea level reconstruction, which is the longest record to date on which
370 this is demonstrated.

371 Our sea-level record shows variability not detected in the record from North Carolina (Kemp
372 et al., 2011) (Supplementary Fig. 1G). This is to be expected given the regionally specific
373 forcing mechanisms of North Atlantic sea levels (Long et al., 2014). For example, along the

374Atlantic seaboard of the southeast USA sea levels may be influenced by the strength and
375position of the Gulf Stream (Ezer et al., 2013, Kopp 2013) and easterly winds are dominant.
376Reconstructions of North Atlantic overturning circulation strength (e.g. Wanamaker et al.,
3772012) display little correspondence with our sea-level record.

378

3795.3 West Icelandic sea level and other driving mechanisms

380To evaluate the potential of other driving mechanisms we also consider ocean mass changes,
381GIA, and steric sea-level rise as potential drivers of our Icelandic RSL record. Reductions in
382ice volume of the Greenland and Antarctic ice sheets and mountain glaciers produce a non-
383uniform sea-level response, with the largest sea-level rise observed in far-field locations
384(Mitrovica et al., 2001). Iceland is located too close to Greenland to be sensitive to any
385potential mass changes of the Greenland Ice Sheet. On the other hand, Iceland is in a far-field
386location with respect to Antarctica, but the lack of correlation with other North Atlantic sea-
387level records largely rules out any Antarctic melt signal as a cause of the sea-level variations
388we reconstructed. Although we cannot completely dismiss contributions from mountain
389glaciers, the absence of coherent signals in other sea-level proxy records indicates they would
390have been small or non-existent.

391Our field site is quite far from the major ice fields in Iceland and the magnitude of vertical
392land motion due to changes in ice mass is estimated to be have been small in recent times
393(Árnadóttir et al., 2009) but may have varied in the past. We therefore examined GIA by
394comparing the timing of the periods of rapid sea-level rise with known changes in local ice
395load history in Iceland. Regional data exist from AD 1700 onwards (Supplementary Fig. 1H),
396whereas in the period AD 1400-1700 ice volume changes are largely unconstrained
397(Kirkbride and Dugmore 2008). The ice body most likely to produce crustal loading (and

398hence RSL rise) in the Viðarhólmi region is Langjökull, but data from other regional ice caps
399and glaciers are reported in Supplementary Fig. 1H for completeness. Of the two major
400glacial advances reported by Flowers et al. (2007), one coincides with rising and the other
401with falling sea level in our reconstruction, showing no coherent response of Viðarhólmi sea
402level to Langjökull mass changes. We therefore reject this as a cause of our reconstructed sea-
403level variability. Additionally, there is no obvious correlation between our sea-level
404variability and changes in more distant Icelandic ice masses (Supplementary Fig. 1H), and
405thus no suggestion these provided the forcing mechanism for this variability.

406With regard to thermosteric sea-level rise we hypothesise that reconstructions of sea-surface
407temperature (SST) and sea-floor temperature (SFT) can be used as a proxy for steric sea
408level. We compare our record with two SST records and a SFT from marine core MD99-2275
409(Supplementary Figs. 1I, J), taken from the North Icelandic Shelf (Knudsen et al., 2004; Ran
410et al., 2011; Sicre et al., 2011). Our coastal site and this core site are both dominated by
411Icelandic Coastal Water (Stefánsson and Ólafsson 1991). There is no correspondence between
412the periods of rapid sea-level change and high SST/SFT, suggesting thermosteric effects on
413Viðarhólmi sea level are not significant.

4146 **Conclusions**

415Only a small number of well-dated late Holocene sea-level reconstructions from the North
416Atlantic are presently available, and these exhibit patterns that reflect a combination of local
417and regional signals (e.g. Long et al., 2014). It is important therefore to increase the spatial
418coverage of well dated sequences and to enhance the resolution of the RSL reconstructions
419where possible.

420 This study has improved an existing RSL record from Viðarhólmi salt marsh in western
421 Iceland (Gehrels et al., 2006) by adding age control and by developing new quantitative sea-
422 level reconstructions based on diatoms. Its main conclusions are as follows:

4231) As shown in many other coastal locations, diatoms perform well as a sea-level proxy,
424 due to their high species diversity, strong elevation control and frequent species turnover.

4252) The careful application of the optimal microfossil group (here, diatoms) can improve
426 RSL reconstructions, but such work must proceed in tandem with the construction of precise
427 age models. We developed a new age model for Viðarhólmi using a combination of AMS ^{14}C
428 dates, ^{137}Cs , geochemical and magnetic markers, as well as a tephra horizons.

4293) We developed new diatom-based RSL reconstructions, using the modern analogue
430 technique (MAT), to identify and remove samples that have poor contemporary equivalents.
431 After screening our reconstruction shows a ~ 0.6 m overall (non-GIA corrected) RSL rise
432 since AD 1570, and three episodes of rapid RSL when the rate of rise exceeded 1.7 mm/yr:
433 AD 1620-1650, AD 1780-1850 and AD 1950-2000.

4344) We hypothesise that Icelandic sea-level variability is controlled by changes in wind
435 patterns associated with shifts in NAO phase based on the strong correlation between a
436 reconstructed NAO index (Trouet et al., 2009) and our detrended RSL record. This result is
437 supported by a positive correlation of the Reykjavik tide-gauge record with regional air
438 pressure and wind speed. NAO-related wind patterns generate set-up on the west coast of
439 Iceland thereby raising local sea level. Taking into account the potential impact of NAO on
440 Icelandic sea level will enhance future predictions of sea-level changes in this region.

4415) The fluctuating nature of the Icelandic RSL record contrasts with other records from
442the North Atlantic and highlights the importance of regionally specific driving mechanisms
443over centennial timescales.

4448 **Acknowledgements**

445 This research was funded by the Natural Environment Research Council (grant no.
446 NE/G003440/1). Radiocarbon dating was performed with help from the Natural Environment
447 Research Council Radiocarbon Committee (allocations 1490.0810 and 1604.0112).
448 Tephrochronology was performed with support from the Tephrochronology Analytical Unit
449 (allocation TAU71/1011). We thank James Scourse and an anonymous reviewer for their
450 constructive comments. We thank Chris Hayward and Donald Herd for help with the tephra
451 analyses, and Gudrun Larsen for advice and for a reference sample of Katla 1721 ash. We
452 thank the Icelandic Met Office for supplying climate data. We thank Peter Schmidt and Björn
453 Lund for advice on GIA and William Marshall for assistance in the field. The paper is a
454 contribution to IGCP project 588 (“Preparing for Coastal Change”) and to PALSEA2 (an
455 INQUA International Focus Group and a PAGES working group).

456

457

- 459 Andersson, H.C., 2002. Influence of long-term regional and large-scale atmospheric
460 circulation on the Baltic sea level. *Tellus A* 54, 76-88.
- 461 Angelier, J., Slunga, R., Bergerat, F., Stefansson, R., Homberg, C., 2004. Perturbation of
462 stress and oceanic rift extension across transform faults shown by earthquake focal
463 mechanisms in Iceland. *Earth Planet. Sci. Lett.* 219, 271-284.
- 464 Angell, J.K., Korshover, T., 1974. Quasi-Biennial and Long-Term Fluctuations in the Centers
465 of Action. *Mon. Weath. Rev.* 102, 669-678.
- 466 Árnadóttir, T., Lund, B., Jiang, W., Geirsson, H., Björnsson, H., Einarsson, P., Sigurdsson, T.,
467 2009. Glacial rebound and plate spreading: results from the first countrywide GPS
468 observations in Iceland. *Geophys. J. Int.* 177, 691-716.
- 469 Barlow, N.L.M., Shennan, I., Long, A.J., 2012. Relative sea-level response to Little Ice Age
470 ice mass change in south central Alaska: Reconciling model predictions and geological
471 evidence. *Earth Planet. Sci. Lett.* 315–316, 62-75.
- 472 Barlow, N.L.M., Shennan, I., Long, A.J., Gehrels, W.R., Saher, M.H., Woodroffe, S.A.,
473 Hillier, C., 2013. Salt marshes as late Holocene tide gauges. *Glob. Planet. Change* 106,
474 90-110.
- 475 Barlow, N.L.M., Long, A.J., Saher, M.H., Gehrels, W.R., Garnett, M.H., Scaife, R.G., 2014.
476 Salt-marsh reconstructions of relative sea-level change in the North Atlantic during the
477 last 2000 years. *Quat. Sci. Rev.* 99, 1-16.
- 478 Birks, H.J.B., Line, J.M., Juggins, S., Stevenson, A.C., Braak, C.J.F.T., 1990. Diatoms and
479 pH reconstruction. *Phil. Trans. Roy. Soc. Lond. B, Biol. Sci.* 327, 263-278.
- 480 Björnsson, H., 1979. Glaciers in Iceland. *Jökull* 29, 74-80.
- 481 Blaauw, M., Christen, J.A., 2011. Flexible paleoclimate age-depth models using an
482 autoregressive gamma process. *Bayesian Anal.* 6, 457-474.
- 483 Brain, M.J., Long, A.J., Woodroffe, S.A., Petley, D.N., Milledge, D.G., Parnell, A.C., 2012.
484 Modelling the effects of sediment compaction on salt marsh reconstructions of recent
485 sea-level rise. *Earth. Planet. Sci. Letts.* 345–348, 180-193.
- 486 Bronk Ramsey, C., Gigham, T., Leach, P., 2004. Towards high-precision AMS; progress and
487 limitations. *Radiocarbon* 46, 17-24.
- 488 Carleton, A.M., 1988. Meridional Transport of Eddy Sensible Heat in Winters Marked by
489 Extremes of the North Atlantic Oscillation, 1948/49–1979/80. *J. Clim.* 1, 212-223.
- 490 Charman, D.J., Gehrels, W.R., Manning, C., Sharma, C., 2010. Reconstruction of recent sea-
491 level change using testate amoebae. *Quat. Res.* 73, 208-219.
- 492 Church, J.A., White, N.J., 2006. A 20th century acceleration in global sea-level rise.
493 *Geophys. Res. Lett.* 33. L01602, doi:10.1029/2005GL024826.
- 494 Compo, G.P., Whitaker, J.S., Sardeshmukh, P.D., Matsui, N., Allan, R.J., Yin, X., Gleason,
495 B.E., Vose, R.S., Rutledge, G., Bessemoulin, P., Brönnimann, S., Brunet, M.,
496 Crouthamel, R.I., Grant, A.N., Groisman, P.Y., Jones, P.D., Kruk, M.C., Kruger, A.C.,
497 Marshall, G.J., Maugeri, M., Mok, H.Y., Nordli, Ø., Ross, T.F., Trigo, R.M., Wang,
498 X.L., Woodruff, S.D., Worley, S.J., 2011. The Twentieth Century Reanalysis Project.
499 *Quart. J. Roy. Meteorol. Soc.* 137, 1-28.
- 500 Cook, E.R., D'Arrigo, R.D., Mann, M.E., 2002. A well-verified, multiproxy reconstruction of
501 the Winter North Atlantic Oscillation Index since A.D. 1400. *J. Clim.* 15, 1754-1764.
- 502 Cornes, R.C., Jones, P.D., Briffa, K.R., Osborn, T.J., 2013. Estimates of the North Atlantic
503 Oscillation back to 1692 using a Paris–London westerly index. *Int. J. Climat.* 33, 228-
504 248.

505 Davies, S.M., Elmquist, M., Bergman, J., Wohlfarth, B., Hammarlund, D., 2007.
506 Cryptotephra sedimentation processes within two lacustrine sequences from west
507 central Sweden. *The Holocene* 17, 319-330.

508 De Rijk, S., 1995. Agglutinated foraminifera as indicators of salt-marsh development in
509 relation to late Holocene sea level rise (Great Marshes at Barnstable, Massachusetts).
510 PhD thesis, Free University, Amsterdam, Netherlands.

511 Douglas, B.C., 2008. Concerning evidence for fingerprints of glacial melting. *J. Coast. Res.*
512 24, 218-227.

513 Einarsson, E.H., Larsen, G., Pórarinnsson, S., 1980. The Sólheimar tephra layer and the Katla
514 eruption of 1357. *Acta Naturalia Islandica* 28, 1-24.

515 Einarsson, M.A., 1984. Climate of Iceland. *World Survey of Climatology* 15, 673-697.

516 Ezer, T., Atkinson, L.P., Corlett, W.B., Blanco, J.L., 2013. Gulf Stream's induced sea level
517 rise and variability along the U.S. mid-Atlantic coast. *J. Geophys. Res. Oceans* 118,
518 685-697.

519 Flowers, G.E., Björnsson, H., Geirsdóttir, Á., Miller, G.H., Clarke, G.K.C., 2007. Glacier
520 fluctuation and inferred climatology of Langjökull ice cap through the Little Ice Age.
521 *Quat. Sci. Rev.* 26, 2337-2353.

522 Foged, N., 1974. Freshwater diatoms in Iceland. *Bibliotheca Phycologica* 15, 1-118.

523 Frankcombe, L.M., Dijkstra, H.A., 2009. Coherent multidecadal variability in North Atlantic
524 sea level. *Geophys. Res. Lett.* 36, L15604, doi:10.1029/2009GL039455.

525 Gehrels, W.R., 1999. Middle and Late Holocene sea-level changes in eastern Maine
526 reconstructed from foraminiferal saltmarsh stratigraphy and AMS ¹⁴C dates on basal
527 peat. *Quat. Res.* 52, 350-359.

528 Gehrels, W.R., Belknap, D.F., Black, S., Newnham, R.M., 2002. Rapid sea-level rise in the
529 Gulf of Maine, USA, since AD 1800. *The Holocene* 12, 383-389.

530 Gehrels, W.R., Marshall, W.A., Gehrels, M.J., Larsen, G., Kirby, J.R., Eiriksson, J.,
531 Heinemeier, J., Shimmield, T., 2006. Rapid sea-level rise in the North Atlantic Ocean
532 since the first half of the nineteenth century. *The Holocene* 16, 949-965.

533 Gehrels, W.R., Milne, G.A., Kirby, J.R., Patterson, R.T., Belknap, D.F., 2004. Late Holocene
534 sea-level changes and isostatic crustal movements in Atlantic Canada. *Quat. Int.* 120,
535 79-89.

536 Gehrels, W.R., Roe, H.M., Charman, D.J., 2001. Foraminifera, testate amoebae and diatoms
537 as sea-level indicators in UK saltmarshes: a quantitative multiproxy approach. *J. Quat.*
538 *Sci.* 16, 201-220.

539 Gehrels, W.R., Woodworth, P.L., 2013. When did modern rates of sea-level rise start? *Glob.*
540 *Planet. Change.* 100, 263-277.

541 Glueck, M.F., Stockton, C.W., 2001. Reconstruction of the North Atlantic Oscillation, 1429–
542 1983. *Int. J. Climatol.* 21, 1453-1465.

543 Haflidason, H., Eiriksson, J., Kreveld, S.V., 2000. The tephrochronology of Iceland and the
544 North Atlantic region during the Middle and Late Quaternary: a review. *J. Quat. Sci.* 15,
545 3-22.

546 Haflidason, H., Larsen, G., Ólafsson, G., 1992. The Recent Sedimentation History of
547 Thingvallavatn, Iceland. *Oikos* 64, 80-95.

548 Haigh, I., Nicholls, R., Wells, N., 2010. Assessing changes in extreme sea levels: Application
549 to the English Channel, 1900–2006. *Cont. Shelf Res.* 30, 1042-1055.

550 Hameed, S., Piontkovski, S., 2004. The dominant influence of the Icelandic Low on the
551 position of the Gulf Stream northwall. *Geophys. Res. Lett.* 31, L09303.

552 Hartley, B., Barber, H.G., Carter, J.R., 1996. *An Atlas of British Diatoms*. Biopress, Bristol,
553 601 pp

554Hayward, C., 2012. High spatial resolution electron probe microanalysis of tephtras and melt
555 inclusions without beam-induced chemical modification. *The Holocene* 22, 119-125.

556Hemphill-Haley, E., 1993. Taxonomy of recent and fossil (Holocene) diatoms
557 (Bacillariophyta) from northern Willapa Bay, Washington. U.S. Department of the
558 Interior, US Geological Survey, 151 pp.

559Hong, B.G., Sturges, W., Clarke, A.J., 2000. Sea Level on the U.S. East Coast: decadal
560 variability caused by open ocean wind-curl forcing. *J. Phys. Ocean.* 30, 2088-2098.

561Hurrell, J., Van Loon, H., 1997. Decadal variations in climate associated with the North
562 Atlantic Oscillation. *Clim. Chan.* 36, 301-326.

563Hurrell, J.W., Kushnir, Y., Ottersen, G., Visbeck, M., 2003. An overview of the North Atlantic
564 oscillation. *Geophys. Mon. Amer. Geophys. Union* 134, 1-36.

565Hustedt, F., 1953. Die Systematik der Diatomeen in ihren Beziehungen zur Geologie und
566 Okologie nebst einer Revision des Halobien-systems. *Svensk Botanisk Tidskrift* 47,
567 509-519.

568Ingólfsson, Ó., Norddahl, H., 2001. High relative sea level during the Bolling Interstadial in
569 western Iceland: A reflection of ice-sheet collapse and extremely rapid glacial
570 unloading. *Arct. Antar. Alp. Res.* 231-243.

571Jackson, S.T., Williams, J.W., 2004. Modern analogs in Quaternary paleoecology: here today,
572 gone yesterday, gone tomorrow? *Ann. Rev. Earth Planet. Sci.* 32, 495-537.

573Jevrejeva, S., Grinsted, A., Moore, J.C., Holgate, S., 2006. Nonlinear trends and multiyear
574 cycles in sea level records. *J. Geophys. Res.* 111, C09012, doi:10.1029/2005JC003229.

575Jevrejeva, S., Moore, J.C., Grinsted, A., 2008. Relative importance of mass and volume
576 changes to global sea level rise. *J. Geophys. Res.* 113, D08105,
577 doi:10.1029/2007JD009208.

578Jones, P.D., Jonsson, T., Wheeler, D., 1997. Extension to the North Atlantic oscillation using
579 early instrumental pressure observations from Gibraltar and south-west Iceland. *Int. J.*
580 *Climat.* 17, 1433-1450.

581Juggins, S., 2003. C2 user guide. Software for ecological and palaeoecological data analysis
582 and visualisation. University of Newcastle, Newcastle upon Tyne, UK.

583Kemp, A.C., Horton, B.P., Corbett, D.R., Culver, S.J., Edwards, R.J., van de Plassche, O.,
584 2009. The relative utility of foraminifera and diatoms for reconstructing late Holocene
585 sea-level change in North Carolina, USA. *Quat. Res.* 71, 9-21.

586Kemp, A.C., Horton, B.P., Donnelly, J.P., Mann, M.E. Vermeer, M., Rahmstorf, S., 2011.
587 Climate related sea-level variations over the past two millennia. *Proc. Nat. Acad. Sci.*
588 108, 11017-11022.

589Kemp, A.C., Horton, B.P., Vane, C.H., Bernhardt, C.E., Corbett, D.R., Engelhart, S.E.,
590 Anisfeld, S.C., Parnell, A.C., Cahill, N., 2013. Sea-level change during the last 2500
591 years in New Jersey, USA. *Quat. Sci. Rev.* 81, 90-104.

592Kirkbride, M.P., Dugmore, A.J., 2008. Two millennia of glacier advances from southern
593 Iceland dated by tephrochronology. *Quat. Res.* 70, 398-411.

594Knudsen, K.L., Eiríksson, J., Jansen, E., Jiang, H., Rytter, F., Gudmundsdóttir, R.E., 2004.
595 Palaeoceanographic changes off North Iceland through the last 1200 years:
596 foraminifera, stable isotopes, diatoms and ice rafted debris. *Quat. Sci. Rev.* 23, 2231-
597 2246.

598Kolker, A.S., Hameed, S., 2007. Meteorologically driven trends in sea level rise. *Geophys.*
599 *Res. Lett.* 34, L23616.

600Kopp, R.E., 2013. Does the mid-Atlantic United States sea level acceleration hot spot reflect
601 ocean dynamic variability? *Geophys. Res. Lett.* 40, 3981-3985.

602Larsen, G., 2000. Holocene eruptions within the Katla volcanic system, south Iceland:
603 Characteristics and environmental impact. *Jökull* 49, 1-28.

604 Long, A.J., Woodroffe, S.A., Milne, G.A., Bryant, C.L., Simpson, M.J.R., Wake, L.M., 2012.
605 Relative sea-level change in Greenland during the last 700 yrs and ice sheet response to
606 the Little Ice Age. *Earth Planet. Sci. Letts.* 315–316, 76-85.

607 Long, A.J., Barlow, N.L.M., Gehrels, W.R., Saher, M.H., Woodworth, P.L., Scaife, R.G.,
608 Brain, M.J., Cahill, N., 2014. Contrasting records of sea-level change in the eastern
609 and western North Atlantic during the last 300 years. *Earth Planet. Sci. Lett.* 388, 110-
610 122.

611 Luterbacher, J., Schmutz, C., Gyalistras, D., Xoplaki, E., Wanner, H., 1999. Reconstruction of
612 monthly NAO and EU indices back to AD 1675. *Geophys. Res. Lett.* 26, 2745-2748.

613 Luterbacher, J., Xoplaki, E., Dietrich, D., Jones, P.D., Davies, T.D., Portis, D.,
614 Gonzalez-Rouco, J.F., von Storch, H., Gyalistras, D., Casty, C., Wanner, H., 2001.
615 Extending North Atlantic oscillation reconstructions back to 1500. *Atmos. Sci. Lett.* 2,
616 114-124.

617 Miller, L., Douglas, B.C., 2007. Gyre-scale atmospheric pressure variations and their relation
618 to 19th and 20th century sea level rise. *Geophys. Res. Lett.* 34., L16602,
619 doi:10.1029/2007GL030862.

620 Milne, G.A., Gehrels, W.R., Hughes, C.W., Tamisiea, M.E., 2009. Identifying the causes of
621 sea-level change. *Nat. Geosci.* 2, 471 - 478.

622 Mitrovica, J.X., Tamisiea, M.E., Davis, J.L., Milne, G.A., 2001. Recent mass balance of polar
623 ice sheets inferred from patterns of global sea-level change. *Nature* 409, 1026-1029.

624 Óladóttir, B., Sigmarsson, O., Larsen, G., Thordarson, T., 2008. Katla volcano, Iceland:
625 magma composition, dynamics and eruption frequency as recorded by Holocene tephra
626 layers. *Bulletin of Volcanology* 70, 475-493.

627 Overpeck, J.T., Webb III, T., Prentice, I.C., 1985. Quantitative interpretation of fossil pollen
628 spectra: Dissimilarity coefficients and the method of modern analogs. *Quat. Res.* 23,
629 87-108.

630 Palmer, A.J., Abbott, W.H., 1986. Diatoms as indicators of sea level change. In: Van de
631 Plassche, O. (Ed.), *Sea Level Research: a Manual for the Collection and Evaluation*
632 *of Data.* Geobooks, Norwich, pp. 457-488.

633 Patterson, R.T., Hutchinson, I., Guilbault, J.P., Clague, J.J., 2000. A comparison of the
634 vertical zonation of diatom, foraminifera, and macrophyte assemblages in a coastal
635 marsh; implications for greater paleo-sea level resolution. *Micropaleontology* 46, 229-
636 244.

637 Ponte, R.M., 1992. The sea level response of a stratified ocean to barometric pressure forcing.
638 *J. Phys. Oceanogr.* 22, 109-113.

639 Ran, L., Jian, g H., Knudsen, K.L., Eiríksson, J., 2011. Diatom-based reconstruction of
640 palaeoceanographic changes on the North Icelandic shelf during the last millennium.
641 *Palaeogeog. Palaeoclim. Palaeoecol.* 302, 109-119.

642 Reimer, P.J., Baillie, M.G.L., Bard, E., Bayliss, A., Beck, J.W., Blackwell, P.G., Ramsey,
643 C.B., Buck, C.E., Burr, G.S., Edwards, R.L., Friedrich, M., Grootes, P.M., Guilderson,
644 T.P., Hajdas, I., Heaton, T.J., Hogg, A.G., Hughen, K.A., Kaiser, K.F., Kromer, B.,
645 McCormac, F.G., Manning, S.W., Reimer, R.W., Richards, D.A., Southon, J.R., Talamo,
646 S., Turney, C.S.M., van der Plicht, J., Weyhenmeyer, C.E., 2009. IntCal09 and Marine09
647 radiocarbon age calibration curves, 0-50,000 years cal BP. *Radiocarbon* 51, 1111-1150.

648 Reimer, P., Bard, E., Bayliss, A., Beck, J., Blackwell, P., Bronk Ramsey, C., Buck, C., Cheng
649 H., Edwards, R., Friedrich, M., Grootes, P., Guilderson, T., Haflidason, H., Hajdas, I.,
650 Hatté, C., Heaton, T., Hogg, A., Hughen, K., Kaiser, K., Kromer, B., Manning, S., Niu,
651 M., Reimer, R., Richards, D., Scott, E., Southon, J., Turney, C., van der Plicht, J., 2013.
652 IntCal13 and MARINE13 radiocarbon age calibration curves 0-50000 years cal BP.
653 *Radiocarbon* 55, 1869-1887.

654Sahsamanoglou, H.S., 1990. A contribution to the study of action centres in the North
655 Atlantic. *Int. J. Climatol.* 10, 247-261.

656Serreze, M.C., Carse, F., Barry, R.G., Rogers, J.C., 1997. Icelandic Low cyclone activity:
657 climatological features, linkages with the NAO, and relationships with recent changes
658 in the Northern Hemisphere circulation. *J. Climate* 10, 453-464.

659Sicre, M.A., Hall, I.R., Mignot, J., Khodri, M., Ezat, U., Truong, M.X., Eiríksson, J.,
660 Knudsen, K.L., 2011. Sea surface temperature variability in the subpolar Atlantic over
661 the last two millennia. *Paleoceanography* 26, PA4218, doi:10.1029/2011PA002169,

662Sigurgeirsson, M.A., 1992. Gjoskumyndanir a Reykjanesi. MSc Thesis, University of
663 Iceland, 113 pp.

664Simpson, G.L., 2007. Analogue methods in palaeoecology: using the analogue package. *J.*
665 *Stat. Software* 22, 1-29.

666Stefánsson, U., Ólafsson, J., 1991. Nutrients and fertility of Icelandic waters. *Rit Fiskideild.*
667 7, 1-56.

668Ter Braak, C.J.F., Juggins, S., 1993. Weighted averaging partial least squares regression (WA-
669 PLS): an improved method for reconstructing environmental variables from species
670 assemblages. *Hydrobiologia* 269-270, 485-502.

671Ter Braak, C.J.F., Prentice, I.C., 1988. A theory of gradient analysis. *Adv. Ecol. Res.* 34.

672Ter Braak, C.J.F., Smilauer, P., 2002. CANOCO reference manual and CanoDraw for
673 Windows user's guide: software for canonical community ordination (version 4.5).

674Thorarinsson, S., 1974. Vötnin stríð (the fast flowing rivers). Saga Skeiðarárhlaupa og
675 Grímsvatnagosa. Bókaútgáfa Menningarsjóðs, Reykjavík. 254 pp.

676Trouet, V., Esper, J., Graham, N.E., Baker, A., Scourse, J.D., Frank, D.C., 2009. Persistent
677 Positive North Atlantic Oscillation Mode Dominated the Medieval Climate Anomaly.
678 *Science* 324, 78-80.

679Trouet, V., Scourse, J.D., Raible, C.C., 2012. North Atlantic storminess and Atlantic
680 Meridional Overturning Circulation during the last Millennium: reconciling
681 contradictory proxy records of NAO variability. *Glob. Planet. Change* 84-85, 48-55.

682Tsimplis, M.N., Shaw, A.G.P., Flather, R.A., Woolf, D.K., 2006. The influence of the North
683 Atlantic Oscillation on the sea-level around the northern European coasts reconsidered:
684 the thermosteric effects. *Phil. Trans. Roy. Soc. A* 364, 845-856.

685Tsimplis, M.N., Woolf, D.K., Osborn, T.J., Wakelin, S., Wolf, J., Flather, R., Shaw, A.G.P.,
686 Woodworth, P., Challenor, P., Blackman, D., Pert, F., Yan, Z., Jevrejeva, S., 2005.
687 Towards a vulnerability assessment of the UK and northern European coasts: the role of
688 regional climate variability. *Phil. Trans. Roy. Soc. A* 363, 1329-1358.

689Van de Plassche, O., 2000. North Atlantic climate-ocean variations and sea level in Long
690 Island Sound, Connecticut, since 500 cal yr A.D. *Quat. Res.* 53, 89-97.

691Vos, P.C., de Wolf, H., 1993. Diatoms as a tool for reconstructing sedimentary environments
692 in coastal wetlands; methodological aspects. *Hydrobiologia* 269, 285-296.

693Wakelin, S.L., Woodworth, P.L., Flather, R.A., Williams, J.A., 2003. Sea-level dependence on
694 the NAO over the NW European Continental Shelf. *Geophys. Res. Letts.* 30, 1403.

695 Wanamaker, A.D.J., Butler, P.G., Scourse, J.D., Heinemeier, J., Eiríksson, J., Knudsen,
696 K.L., Richardson, C.A., 2012. Surface changes in the North Atlantic meridional
697 overturning circulation during the last millennium. *Nat. Comm.* 3, 899.

698Ward, P.L., 1971. New interpretation of the geology of Iceland. *Geol. Soc. America Bull.* 82,
699 2991-3012.

700Watcham, E.P., Shennan, I., Barlow, N.L.M., 2013. Scale considerations in using diatoms as
701 indicators of sea-level change: lessons from Alaska. *J. Quat. Sci.* 28, 165-179.

702Van der Werff, A., Huls, H., 1957-1974. Diatomeeënflora van Nederland, Reprinted 1976.
703 Otto Koeltz Science Publishers, Koenigstein. West Germany.

704 Woodworth, P.L., Flather, R.A., Williams, J.A., Wakelin, S.L., Jevrejeva, S., 2007. The
705 dependence of UK extreme sea levels and storm surges on the North Atlantic
706 Oscillation. *Cont. Shelf Res.* 27, 935-946.
707 Woolf, D.K., Shaw, A.G., Tsimplis, M.N., 2003. The influence of the North Atlantic
708 Oscillation on sea-level variability in the North Atlantic region. *The Glob. Atmos.*
709 *Ocean Syst.* 9, 145-167. Wunsch, C., Stammer, D., 1997. Atmospheric loading and the
710 oceanic “inverted barometer” effect. *Rev. of Geophys.* 35, 79-107.

711 **Figure captions**

712 **Fig. 1.** Location map and previous work. A: Regional map showing location of study site
713 (Viðarhólmi) and other locations mentioned in text. B: Aerial photograph of Viðarhólmi salt
714 marsh showing location of surface sample transects (T1-4) and sampled section V3A. C:
715 Foraminifera-based sea-level reconstruction for Viðarhólmi salt marsh, with 2σ error bars,
716 spanning the last 2000 years from Gehrels et al. (2006).

717 **Fig. 2.** Stratigraphy and sedimentological data of section V3A, showing dry bulk density
718 (DBD), grain-size fractions and lithology (including dated tephras).

719 **Fig. 3** Transfer function model details. A: Scatter plot of observed *versus* model-predicted
720 elevations of modern diatom samples shown in Fig. 5. B: Residuals (predicted minus
721 observed sample elevations). RMSEP – root mean squared error of prediction.

722 **Fig. 4** Age model and output files computed by the software package Bacon (Blaauw and
723 Christen, 2011) for section V3A. A: Age-depth model based on ^{14}C (purple) and other
724 (turquoise) dates. The red curve shows the weighted mean ages of all depths, whereas
725 greyscales show uncertainties (where darker grey indicates more certain sections). B: Stable
726 Markov Chain Monte Carlo run. C: Prior (green curve; gamma distribution with mean 20,
727 shape 3) and posterior (grey histogram) distributions for the accumulation rate (yr/cm). D:
728 Prior (green curve; beta distribution with strength 3 and mean 0.1) and posterior (grey
729 histogram) for the memory. Section sizes were set at 5 mm.

730 **Fig. 5** The vertical distribution of the main species of diatoms, shown for species greater than
731 5% of total valves counted. Diatom classification according to Vos and de Wolf (1993). P
732 (blue): Polyhalobian; M (green): Mesohalobian (brackish); O-h (light orange):

733 Oligohalobian-halophilous; O-i (dark orange): Oligohalobian-indifferent; H (red):

734 Halophobous. MSL - mean sea level.

735 **Fig. 6** Fossil assemblages of the main species of diatoms used as sea-level proxies. Diatoms
736 shown for species greater than 5% of total valves counted. Diatom classification as in Fig. 5.
737 Palaeo-marsh surface elevations (PMSE) are also shown. Samples with good/close modern
738 analogues are shown as solid circles. Samples with poor modern analogues are shown as
739 open circles.

740 **Fig. 7** New relative sea-level reconstruction for western Iceland based on diatoms. A: New
741 reconstruction for the last half millennium. Black crosses are data point from levels that were
742 directly dated. Grey crosses are data points for which ages are estimated from the age model
743 (Fig. 4). Superimposed is the Reykjavik tide-gauge record (www.psmsl.org). B: Composite
744 RSL reconstruction for western Iceland, combining the diatom-based reconstruction for the
745 last 500 years (this paper) and the foraminifera-based reconstruction for the older part of the
746 record (Gehrels et al., 2006).

747 **Fig. 8** Annual winter mean time series of air pressure, wind speed, wind direction, and NAO
748 index, averaged for the box shown in Fig. 9 over the period 1871-2011. Mean sea level
749 (MSL) at Reykjavik is shown as red lines. Upper panels (A-D) show annual data and lower
750 panels (E-H) show 9-year running averages. Note that the vertical axes in panels A and E are
751 reversed compared to the other panels.

752 **Fig. 9** Detrended mean sea-level (MSL) recorded at Reykjavik, showing sea levels
753 subdivided into four height categories: >1 standard deviation (very high), 0-1 standard
754 deviation (high), -1-0 standard deviation (low), and <-1 standard deviation (very low). Maps
755 show the average air pressure, wind speed and wind direction for each of the four height
756 categories. The box shows the area used to calculate parameters shown in Fig. 8.

757**Fig. 10** Comparison of our sea-level reconstruction with the NAO proxy record of Trouet et
758al. (2009). A: Sea-level reconstruction for western Iceland. The envelope represents the 68%
759confidence limits calculated from chronological and height errors of data points. B: Rates of
760sea-level change for the Icelandic sea-level reconstruction in panel A. The envelope shows
76168% confidence limits and the line represents the most probably reconstruction. The grey
762vertical bars show the three periods where this line exceeds the 20th century average of 1.7
763mm/yr (Church and White 2006). C: The reconstructed NAO index of Trouet et al. (2009).

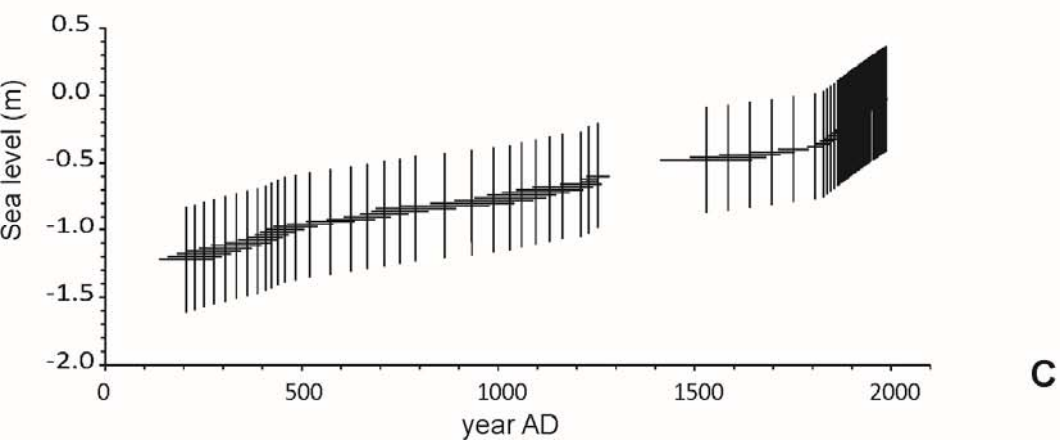
764**Fig. 11** Scatter plot showing the correlation between the detrended sea-level proxy data from
765western Iceland (see Supplementary Figure 1B) and the reconstructed NAO index (Trouet et
766al., 2009).

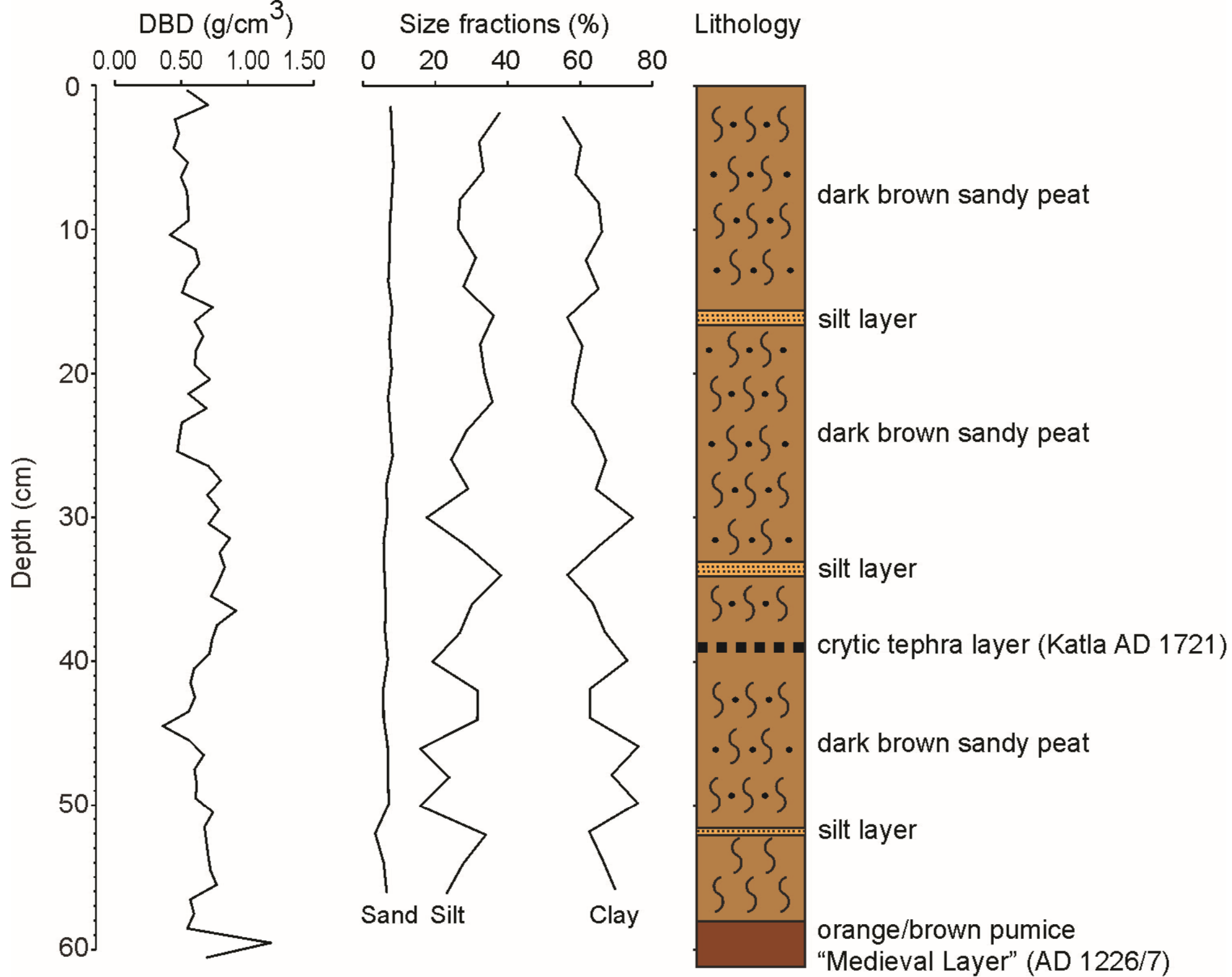
767

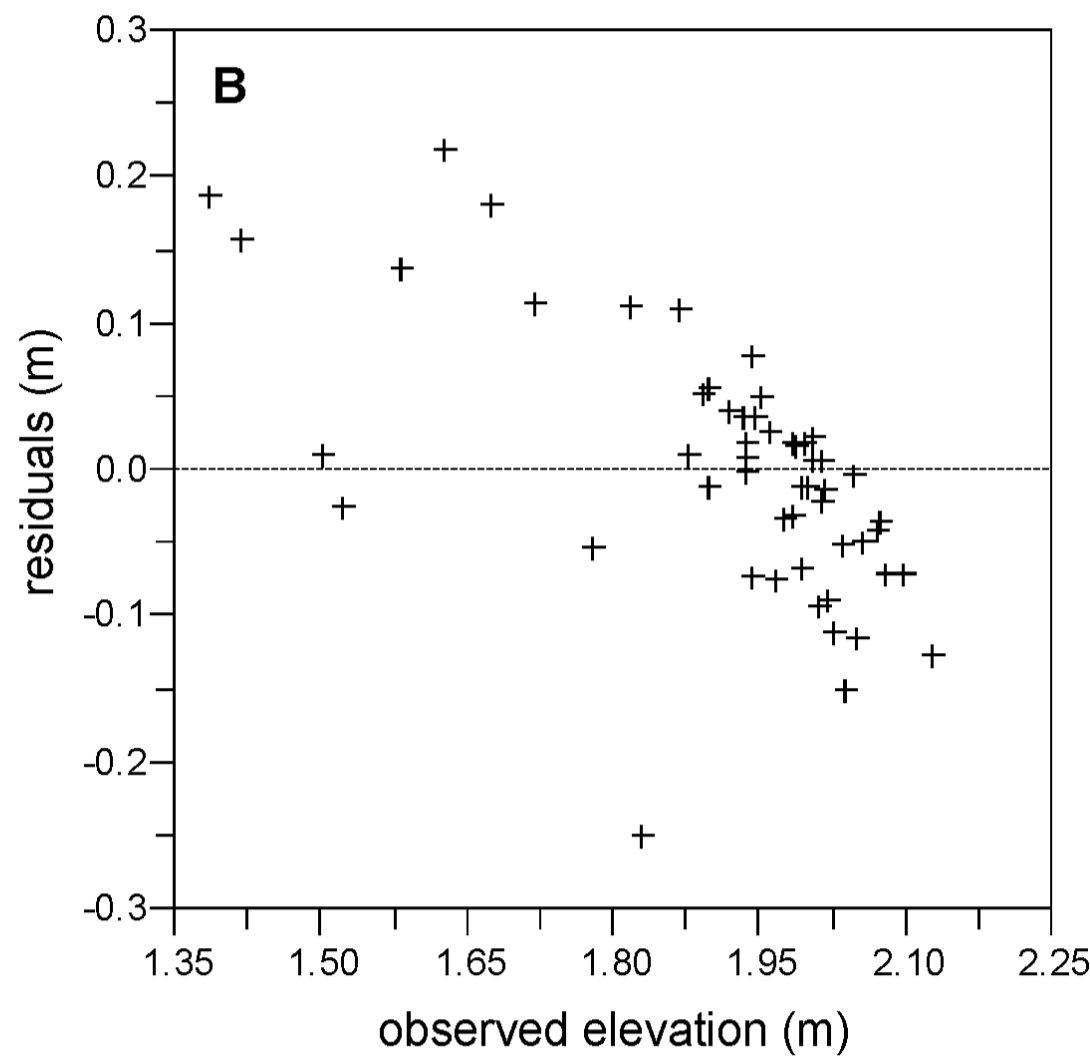
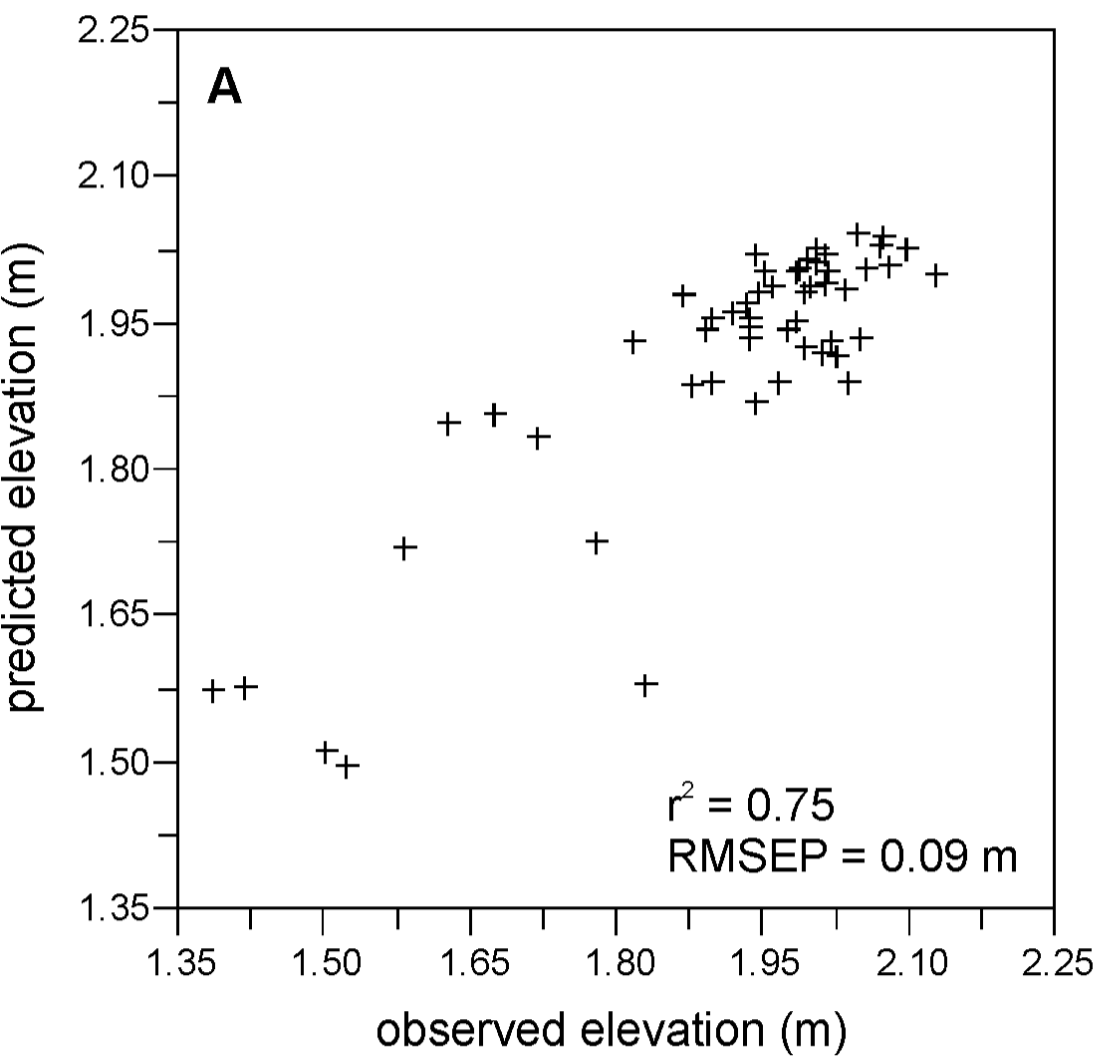
768**Table captions**

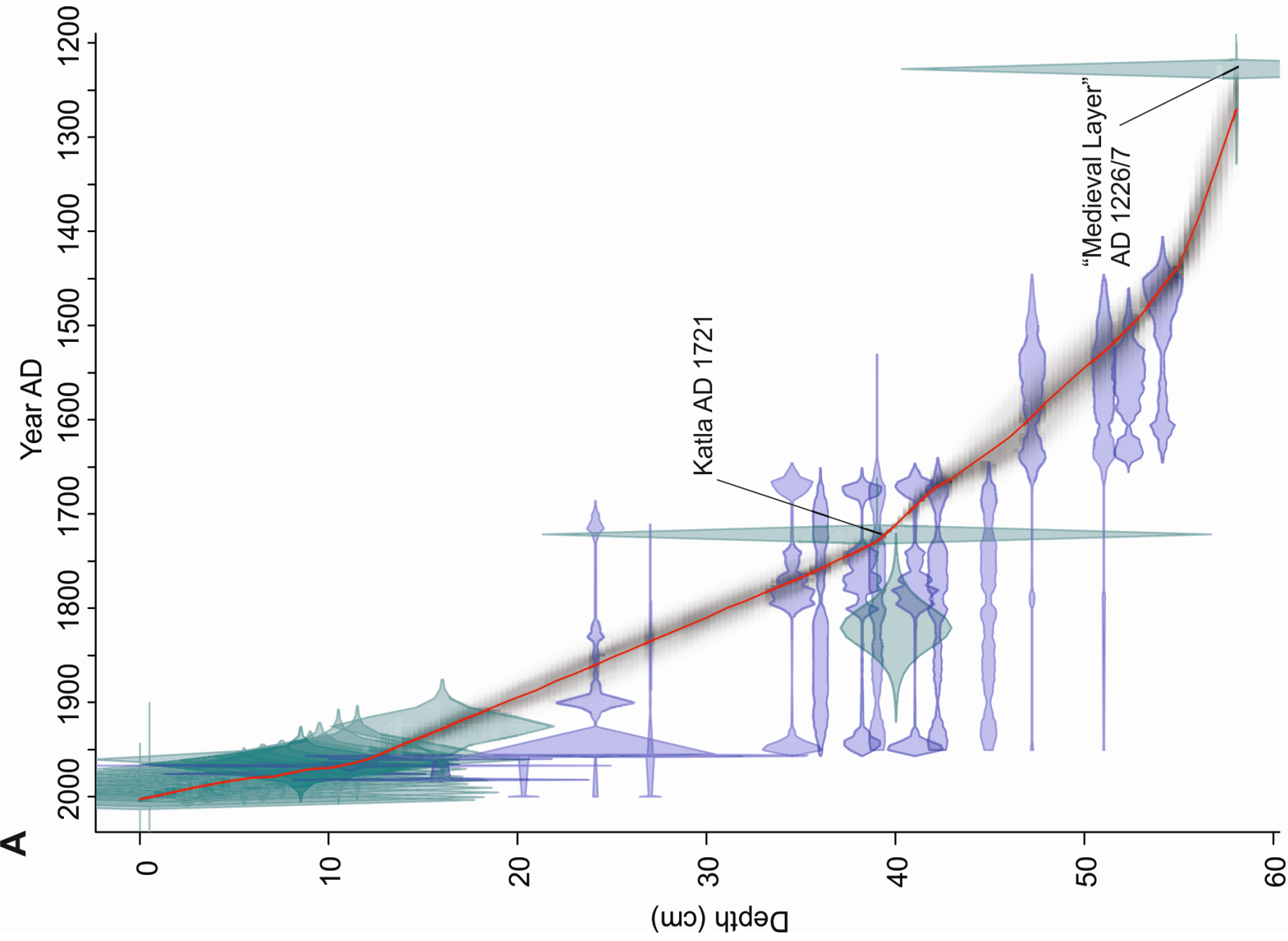
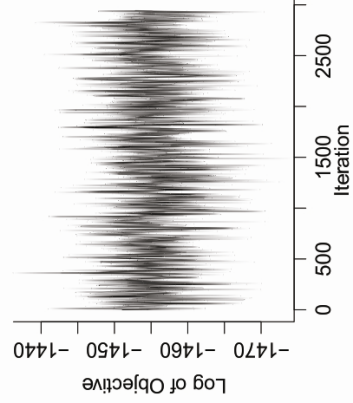
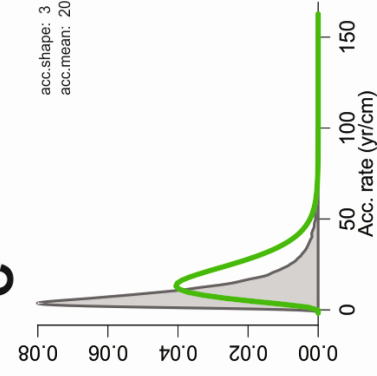
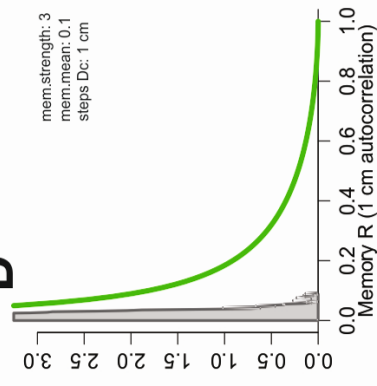
769**Table 1** Age-depth data used to reconstruct relative sea-level changes in western Iceland
770during the last 500 years. Sources: 1 - this study; 2 - Gehrels et al. (2006).

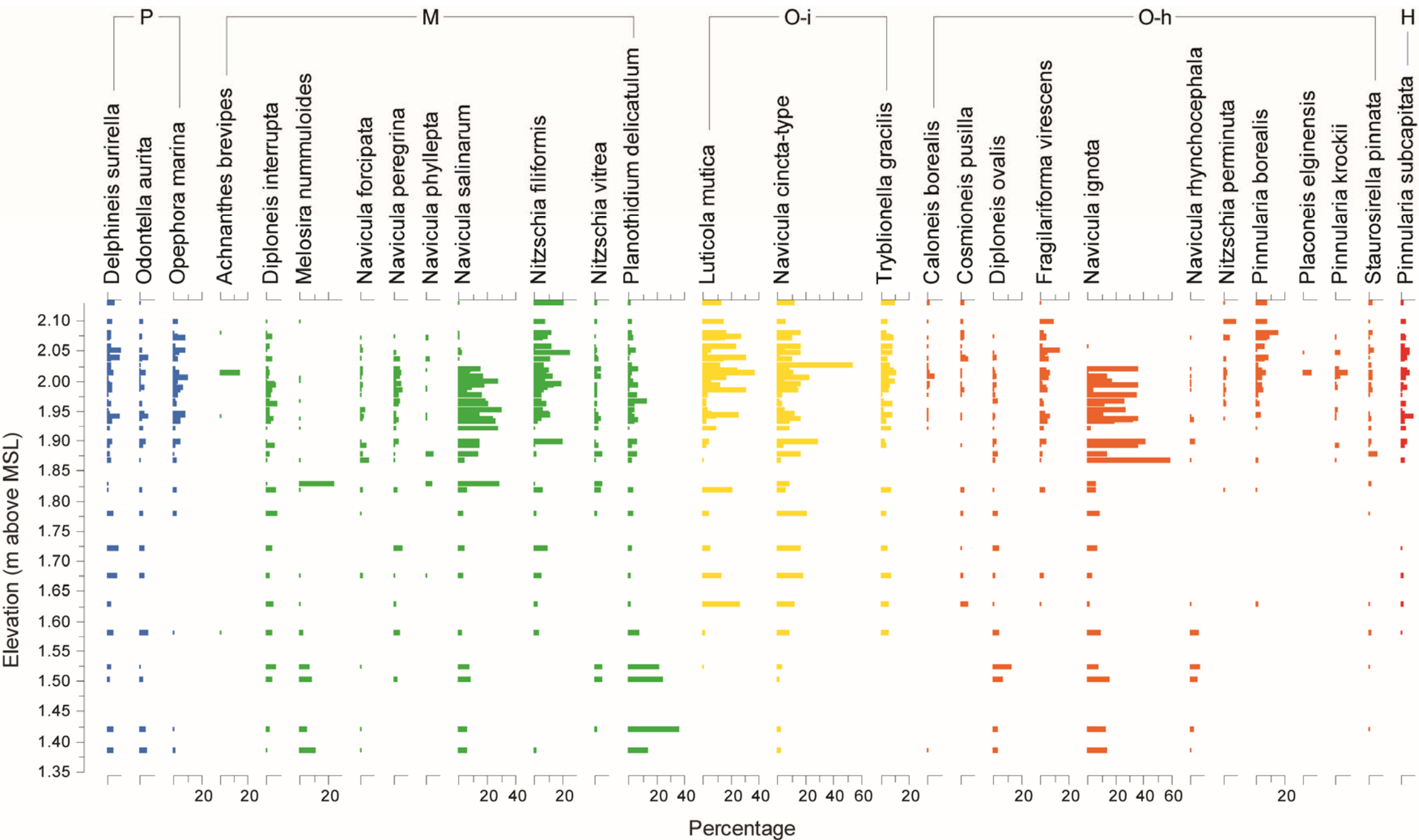
771**Table 2** Icelandic sea-level data for the last 500 years. I.M. – indicative meaning. MSL –
772mean sea level. Relative sea level (RSL) positions are given relative to present sea level (i.e.
7730 m).

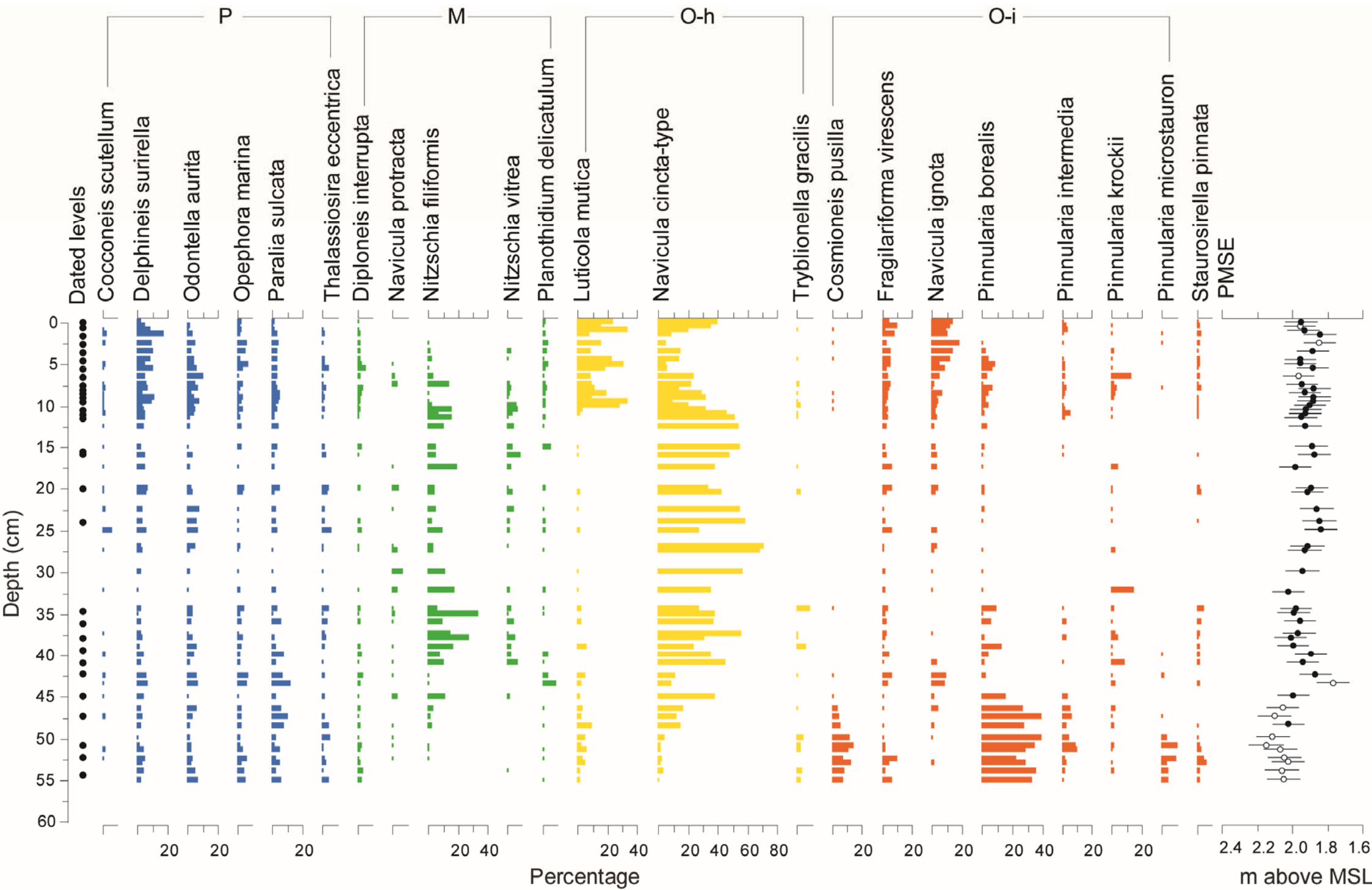


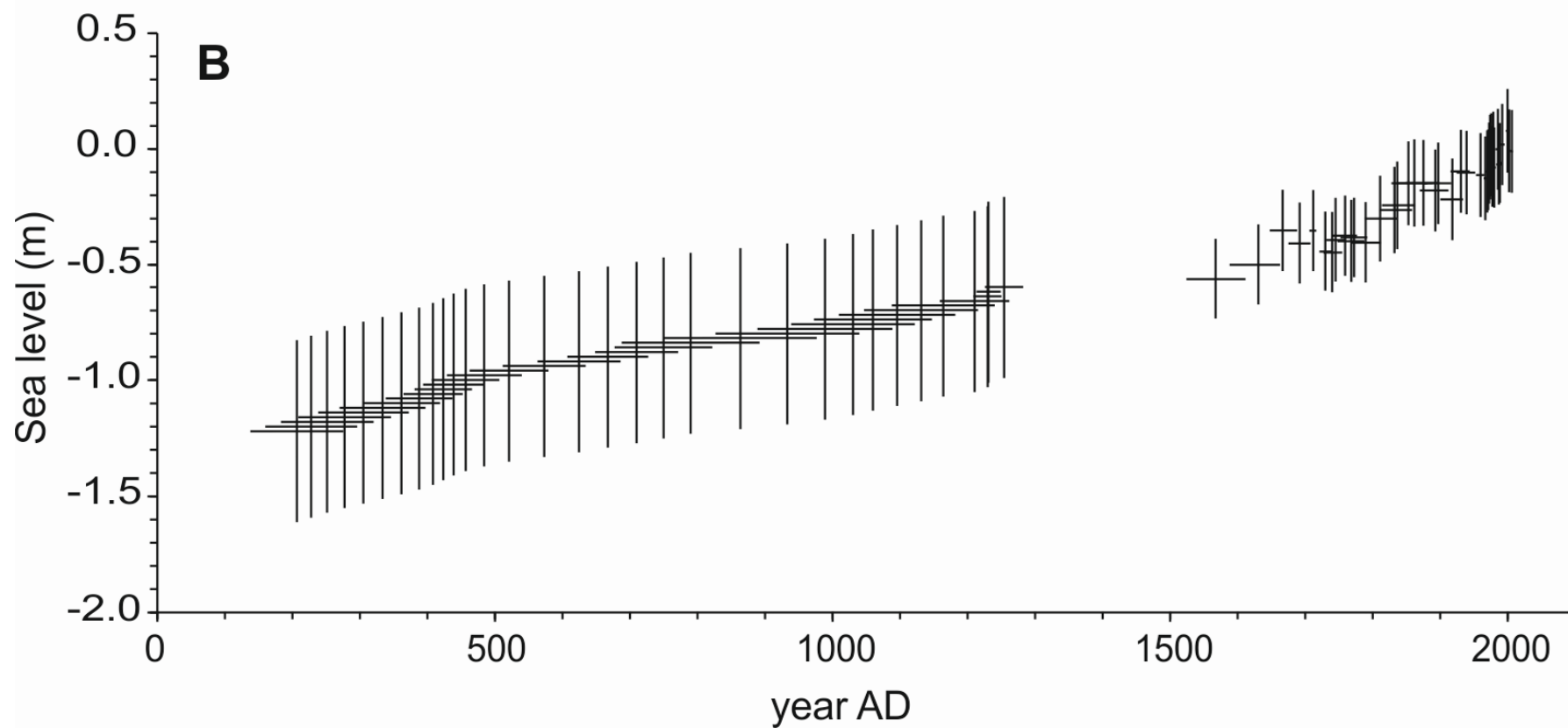
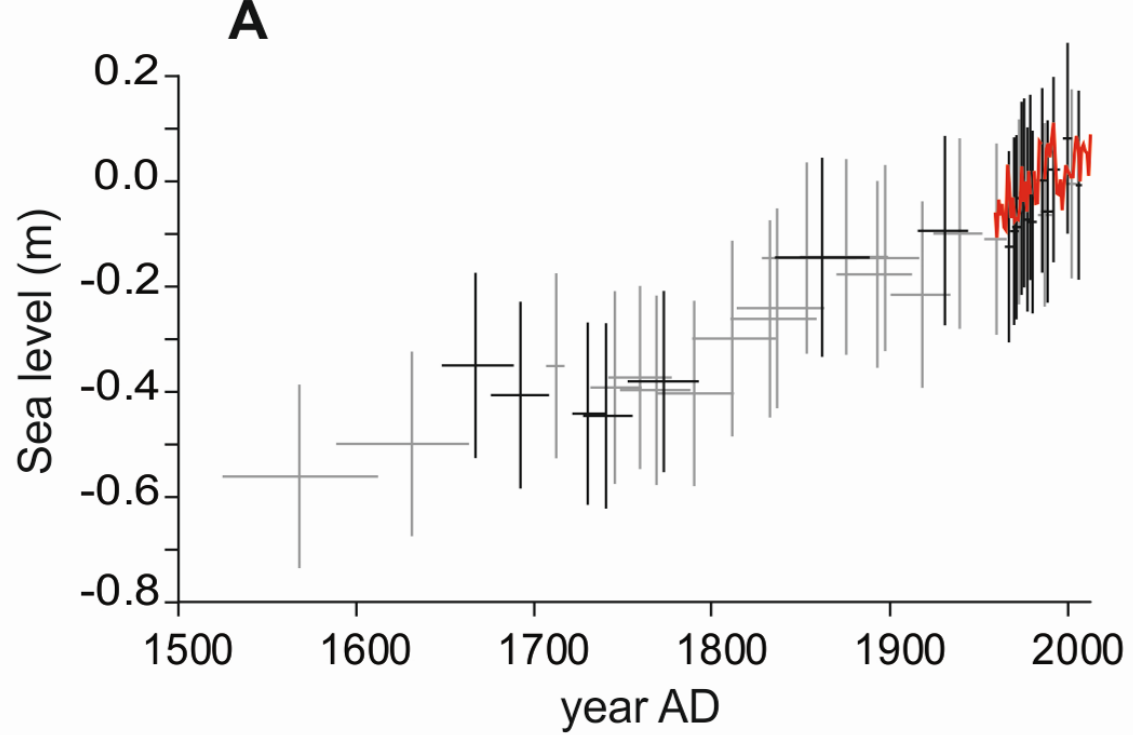




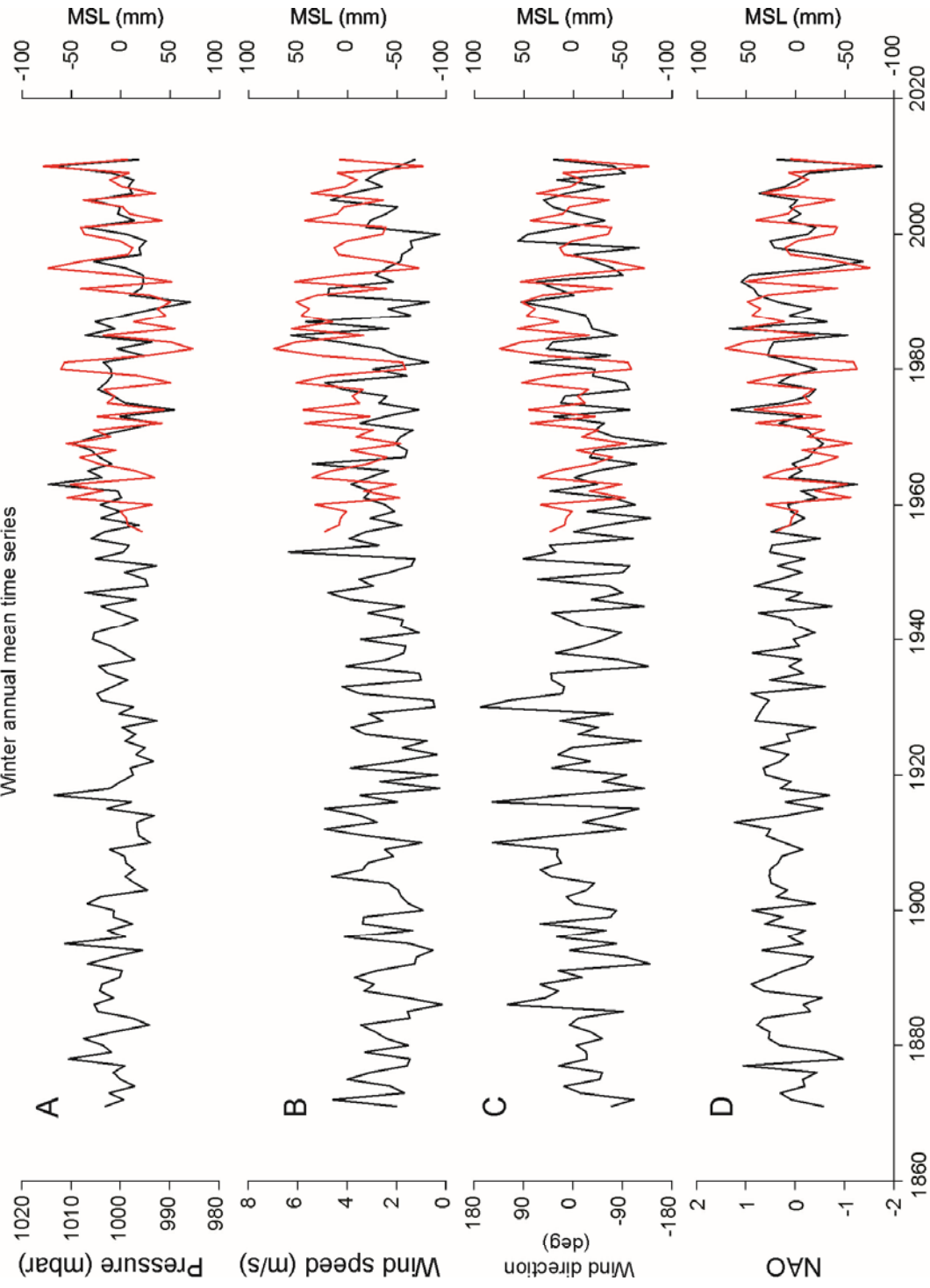
A**B****C****D**



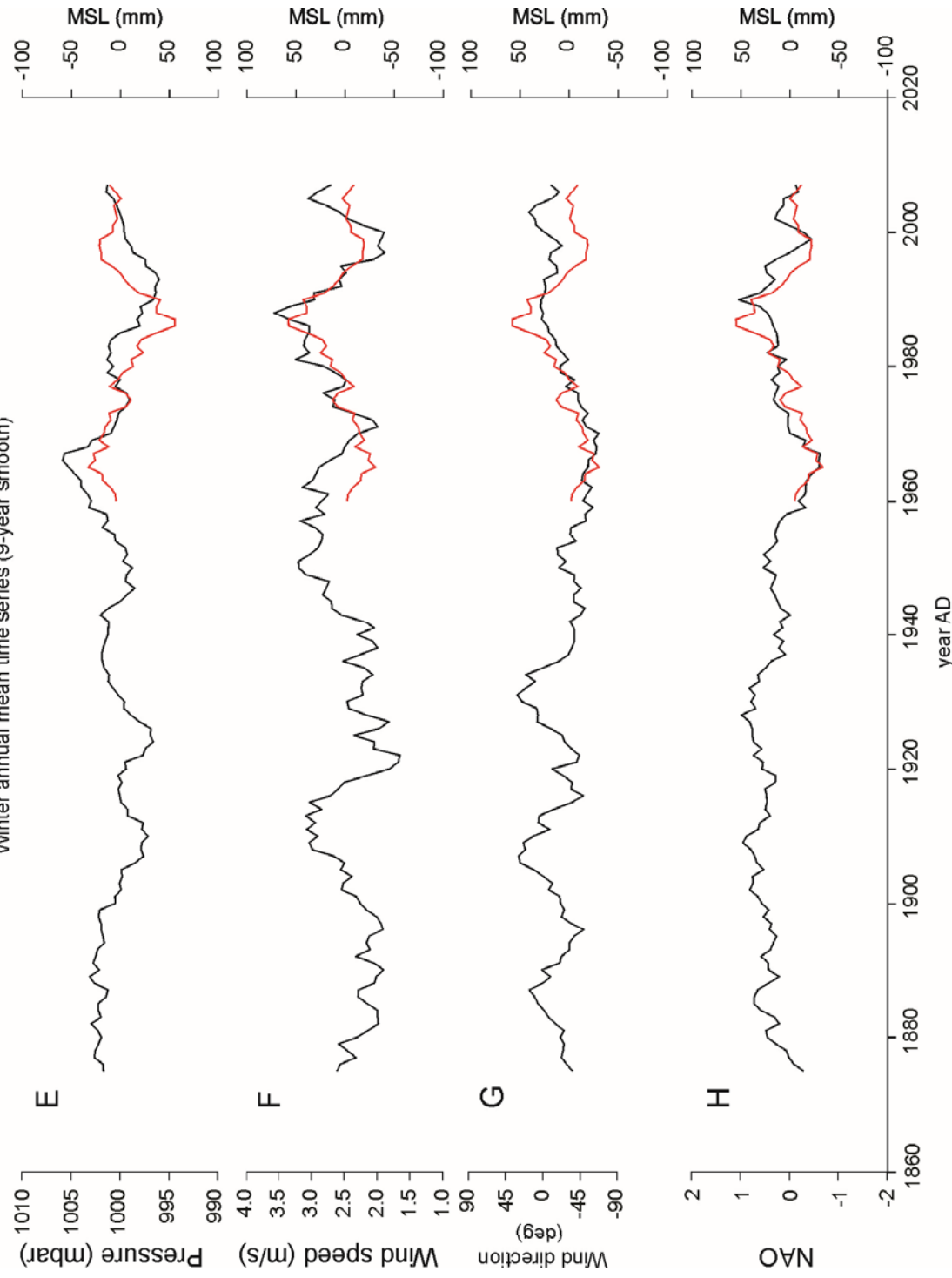




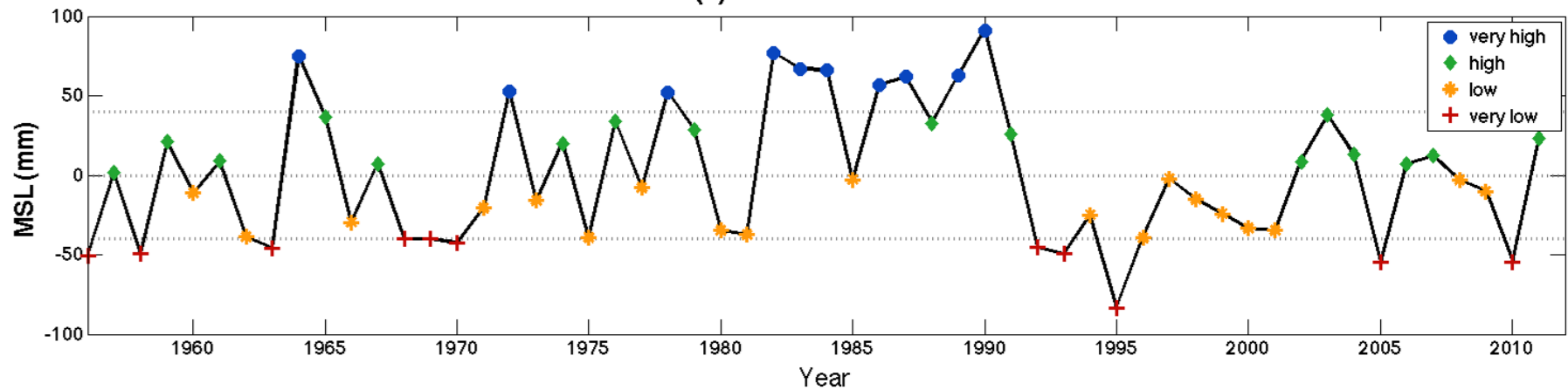
Winter annual mean time series



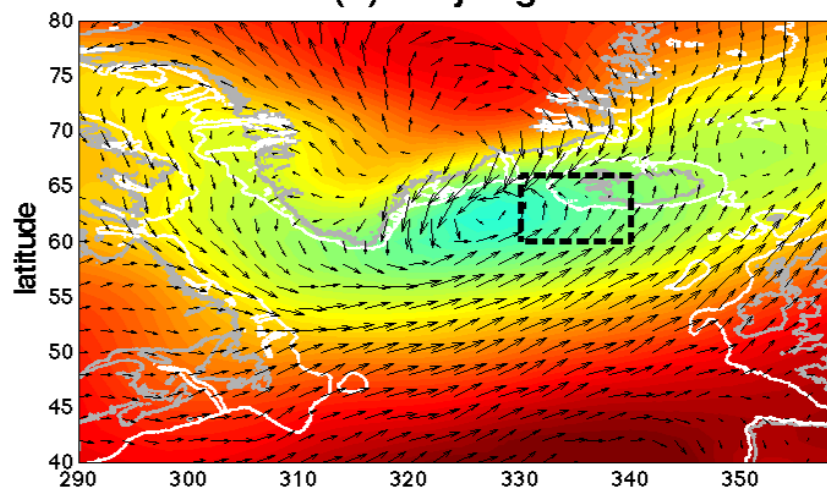
Winter annual mean time series (9-year smooth)



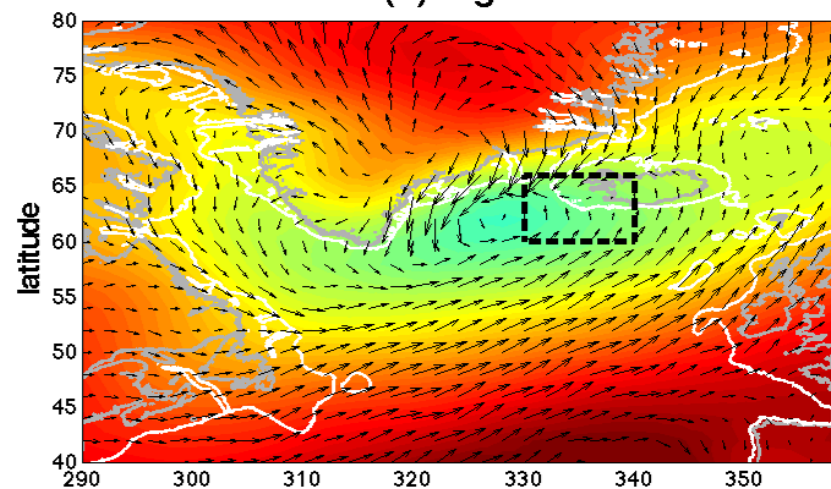
(a) De-trended MSL



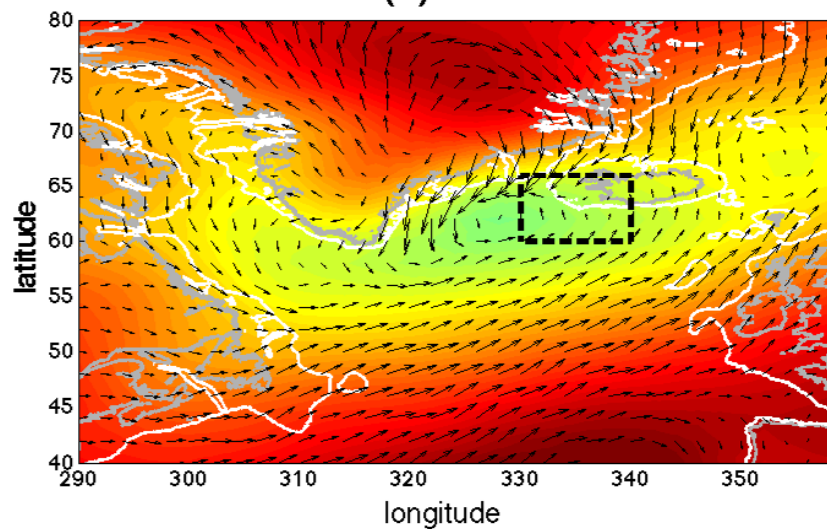
(b) Very High



(c) High



(d) Low



(e) Very Low

